Bose-Einstein Correlations and Classical Transport Models

*N. S. Amelin*and R. Lednicky*[1]
Laboratoire SUBATECH, Université de Nantes, Ecole des Mines de Nantes,
F-44072 Nantes Cedex 03, France LPSTA

[1]*Institute of Physics of the Academy of Sciences of the Czech Republic*
Na Slovance 2, 18040 Prague 8, Czech Republic

*) On leave of absence from the JINR, Dubna, Russia

Abstract

We discuss how to add Bose-Einstein correlations to simulations of ultra-relativistic heavy-ion collisions. We show how to calculate the influence of multi-particle Bose-Einstein correlations not only on the correlation functions of two or more identical spinless bosons, but also on multiplicity distributions and single-particle spectra obtained from an event generator. We also discuss the effect of the Coulomb and the strong interaction in the multi-particle final state. A computer code has been developed for practical calculations. Coupling this code with the parton-string model, we have demonstrated the importance of Bose symmetrization on multi-particle production in ultra-relativistic heavy-ion collisions for different systems of colliding nuclei at initial energy 200 AGeV.

1 Introduction

The multiple particle production in ultra-relativistic heavy-ion and hadronic collisions is studied to understand the production mechanism and to reach finally the conclusions about properties of the nuclear matter under extreme conditions. An important part of these studies is the investigation of particle correlations. The experimental observations indicate substantial contribution of the Bose-Einstein (BE) correlations, which enhance the probability to find two or more identical bosons at low relative momentum. These correlations arise as an interference effect due to the symmetrization requirement on the production amplitude of identical bosons. In particle physics the two-boson interference effects were first observed in $p\bar{p}$ annihilations as an enhanced production of pairs of identical charged pions with small opening angles [1]. In heavy-ion reactions, where hundreds of identical pions and kaons are produced, the multi-boson interference effects can be of far more importance.

An important aspect of the BE correlations is the boson interferometry. Long time ago Kopylov and Podgoretsky [2, 3] observed a deep analogy between interferometry in astronomy and particle physics. Similar to astronomy, they suggested to study the interference effect in terms of the correlation function and presented its simple space-time parameterization. Now this method is widely used to measure the space-time characteristics of the production process. However, for a number of reasons, interferometry in particle physics is more complicated than interferometry in astronomy. There are numerous factors (e.g. the final state interactions, the dynamical correlations between particles, the correlation between their momenta and emission points, resonance decays etc.) which make the direct extraction of the source extent nearly impossible. In particular, the information on space-time development of particle production in heavy-ion collisions can be obtained from the correlation measurements only within a chosen transport model.

The transport models based on the parton, classical string or hydrodynamical approaches are widely used to predict the particle production in ultra-relativistic heavy-ion collisions, to determine the acceptance of detectors and to compare the results obtained in different experiments under different kinematical conditions. They assume that the produced hadrons are on mass-shell, point-like and can be precisely localized in both coordinate and momentum spaces and predict the coordinates and momenta of all particles at all times. Being classical approaches, interference effects are beyond their scope. Since the BE correlations arise due to the interference of the amplitudes of indistinguishable processes, they cannot be taken into account in these models directly.

Since nature includes BE correlations and since they influence the spectra in a non-negligible way, it is necessary to include these correlations into the simulations of the reactions, not only to improve the predictive power of these models but also to verify the information content of the measured spectra on the source of particle emission. This requires the consideration of how to connect a classical theory with the BE correlations.

There are several attempts to include the two-particle BE effects in the simulatios based on classical transport models. These attempts address mainly the two-boson

interferometry (for a recent review see [4]).

In the following, we start with the calculation of the two-boson correlation function within a classical transport model. Then we extend this approach to calculate correlation functions of three or more identical particles. Further we discuss the influence of multi-particle BE correlations on observables like multiplicity distributions, one-particle spectra and two-particle correlation functions. Furthermore we study how other correlations, like the one between the coordinate and momentum space, which are present in transport models, influence the BE correlations. The theoretical considerations are accompanied by the numerical calculations using the parton-string model [5]. This model contains most of the features of the standard Monte-Carlo event generators used to describe the ultra-relativistic heavy-ion collisions and allows to perform calculations in modest computer time. The aim of calculations within this particular model is not to make a comparison with the experimental data and not to improve the model, but to demonstrate practical possibility and necessity of the inclusion of BE and final state interaction effects and to test the developed numerical code, which can then be used within other dynamical models.

The paper is organized now as follows. In Sections 2 and 3 we explain the ideas and assumptions allowing to calculate two-particle correlation functions using simulations based on a classical transport model. In Section 4, we show how to calculate the multi-particle correlations due to Bose symmetrization within such a model. In Section 5, we demonstrate how to calculate different corrections, particularly, for single-particle spectra and multiplicity distribution, connected with inclusion of the multi-particle BE correlations. We also consider the distortion of the two-boson interferometry by multi-boson correlations. Finally, in Section 6, besides the effect of BE statistics, we also discuss how to add the correlations due to the final state Coulomb and strong interactions.

2 Two-boson correlation function: formalism

We start with the process in which, besides the system described by quantum numbers $\{\alpha\}$, only two identical spinless bosons with the 4-momenta $p_1 = (E_1, \mathbf{p}_1)$ and $p_2 = (E_2, \mathbf{p}_2)$ are produced. We introduce the non-symmetrized production amplitude $T(p_1, p_2; \{\alpha\})$ normalized in such a way that, in the case of switched off the effect of BE statistics, the inclusive differential production cross section of the two particles is:

$$E_1 E_2 \frac{d^6\sigma_2}{d^3\mathbf{p}_1 d^3\mathbf{p}_2} = \sigma_2 \sum_{\{\alpha\}} \mid T(p_1, p_2; \{\alpha\}) \mid^2 \equiv \sigma_2 P_2(\mathbf{p}_1, \mathbf{p}_2). \tag{1}$$

Here sum over $\{\alpha\}$, taking into account the conservation laws, represents summation over the discrete quantum numbers and integration over the continuous ones. The

invariant production probability P_2 is normalized to unity as

$$\int \frac{d^3\mathbf{p}_1}{E_1}\frac{d^3\mathbf{p}_2}{E_2}P_2(\mathbf{p}_1,\mathbf{p}_2) = 1. \tag{2}$$

The lower index 2 in the probability P_2 means that here we consider production of only two identical bosons of a given type. The requirement of Bose symmetry leads to the substitution of the production probability P_2 by a symmetrized one:

$$P_2^c(\mathbf{p}_1,\mathbf{p}_2) = \frac{1}{2!}\sum_{\{\alpha\}} \mid [T(p_1,p_2;\{\alpha\}) + T(p_2,p_1;\{\alpha\})] \mid^2 . \tag{3}$$

To introduce the space-time characteristics of the particle production, we will follow Kopylov and Podgoretsky (see, e.g., [2, 3]) and assume that particles are emitted by one-particle sources ($A \to 1, B \to 2$) which are considered as classical so they can be treated by parameters and not by amplitudes. Thus the 4-coordinates of the source centers x_A and x_B and other source characteristics in the model can be considered as a part of the quantum numbers $\{\alpha\} \equiv \{x_A, x_B, \alpha'\}$. It was noticed out by Kopylov and Podgoretsky that the BE correlation is mainly determined by the phase factor $\exp(ip_1x_A + ip_2x_B)$ contained in the amplitude $T(p_1,p_2;\{\alpha\})$. To see this, let us first introduce the production amplitude $\tilde{T}(x_1,x_2;\{\alpha\})$ in space-time representation. Note that, in the case of finite size sources, the 4-coordinates x_1 and x_2 of the particle emission points are different from x_A and x_B (see Fig. 1). For non-interacting particles, this amplitude is related to the amplitude $T(p_1,p_2;\{\alpha\})$ by the usual Fourier transform:

$$T(p_1,p_2;\{\alpha\}) = \int d^4x_1 d^4x_2 \exp(ip_1x_1 + ip_2x_2)\tilde{T}(x_1,x_2;\{\alpha\}). \tag{4}$$

Now, taking into account the translation invariance, we can write

$$\tilde{T}(x_1,x_2;\{\alpha\}) \equiv \tilde{t}(x_1 - x_A, x_2 - x_B;\{\alpha\}). \tag{5}$$

Inserting (5) into (4) and introducing the Fourier transform

$$t(p_1,p_2;\{\alpha\}) = \int d^4\xi_1 d^4\xi_2 \exp(ip_1\xi_1 + ip_2\xi_2)\tilde{t}(\xi_1,\xi_2;\{\alpha\}), \tag{6}$$

we get:

$$T(p_1,p_2;\{\alpha\}) = \exp(ip_1x_A + ip_2x_B)t(p_1,p_2;\{\alpha\}). \tag{7}$$

It is clear from Eq. (6) that the momentum dependence of the amplitude $t(p_1,p_2;\{\alpha\})$ is determined by the space-time extent of the sources. For example, assuming that the sources emit particles independently:

$$\tilde{t}(\xi_1,\xi_2,\{\alpha\}) = u_A(\xi_1)u_B(\xi_2)v(\{\alpha\}) \tag{8}$$

and that the distribution of the emission points in the source rest frame is given by a simple Gaussian

$$u_A(\xi_1) \sim \exp(-\frac{\xi_1^2}{2r_A^2} - \frac{\xi_{01}^2}{2\tau_A^2}), \tag{9}$$

we obtain in the case of resting sources:

$$t(p_1, p_2, \{\alpha\}) \sim \exp(-\frac{1}{2}r_A^2 \mathbf{p}_1^2 - \frac{1}{2}\tau_A^2 p_{01}^2)\exp(-\frac{1}{2}r_B^2 \mathbf{p}_2^2 - \frac{1}{2}\tau_B^2 p_{02}^2) v(\{\alpha\}). \tag{10}$$

The probability $|v(\{\alpha\})|^2$ describes the production of particle sources and depends on the 4-coordinates of the source centers x_A and x_B. Note that Eq. (10) is valid also off mass-shell when $p_{01} \neq E_1$ and $p_{02} \neq E_2$.

Inserting the amplitude (7) into Eq. (1) and separating the integration over x_A and x_B from the sum over the quantum numbers $\{\alpha\} = \{x_A, x_B, \alpha'\}$, we get

$$P_2^c(\mathbf{p}_1, \mathbf{p}_2) = \\ = \int d^4x_A d^4x_B \sum_{\{\alpha'\}} \{| t(p_1, p_2; \{\alpha\}) |^2 + Re[t(p_1, p_2; \{\alpha\}) t^*(p_2, p_1; \{\alpha\}) \exp(iq_{12}x_{AB})]\}, \tag{11}$$

where $q_{12} = p_1 - p_2$ and $x_{AB} = x_A - x_B$. Please, note that $\{p_i, p_j; \alpha\} = \{p_i x_A, p_j x_B; \alpha'\}$, i.e. the source parameters x_A and x_B characterize the emission of the particles with momenta p_i and p_j, respectively. In Eq. (11) we took into account that, after integration and summation over the quantum numbers $\{\alpha\}$, the contributions of the two diagonal terms are equal.

Usually, as shown in Fig. 1, the space-time extent of the sources is assumed much smaller than that of the production region ($r_A \ll r_0$, $\tau_A \ll \tau_0$). In other words, the momentum dependence of the amplitude $t(p_1, p_2; \{\alpha\})$ is assumed unimportant when varying the 4-momenta p_1 and p_2 by the amount characteristic for the interference effect, determined by the inverse size of the production region. Under such a *smoothness* assumption we arrive at the final result of Kopylov-Podgoretsky [2]:

$$P_2^c(\mathbf{p}_1, \mathbf{p}_2) \doteq \int d^4x_A d^4x_B P_2(p_1, x_A; p_2, x_B)[1 + \cos(q_{12}x_{AB})], \tag{12}$$

where

$$P_2(p_1, x_A; p_2, x_B) = \sum_{\{\alpha'\}} | t(p_1, p_2; \{x_A, x_B, \alpha'\}) |^2 \tag{13}$$

represents the classical emission probability. It is normalized by the condition:

$$\int \frac{d^3\mathbf{p}_1}{E_1}\frac{d^3\mathbf{p}_2}{E_2} d^4x_A d^4x_B P_2(p_1, x_A; p_2, x_B) = \int \frac{d^3\mathbf{p}_1}{E_1}\frac{d^3\mathbf{p}_2}{E_2} P_2(p_1, p_2) = 1. \tag{14}$$

Note that the sum over $\{\alpha'\}$ contains the summation over all possible types of the sources. We also note that Eq. (12) becomes exact in the special case of amplitudes with a universal functional dependence on the momenta, when all sources are of the same type (in particular, in the case of universal parameters r_A and τ_A in Eq. (10)) and at rest in a chosen system.

The approximate Eq. (12) allows a simple interpretation. The second factor in the integral is just square of the amplitude corresponding to the emission of the two identical bosons at the points x_A and x_B:

$$1 + \cos(q_{12}x_{AB}) = | \frac{1}{\sqrt{2!}}[\exp(ip_1x_A + ip_2x_B) + \exp(ip_2x_A + ip_1x_B)] |^2 . \tag{15}$$

The finite source sizes still reveal themselves in the momentum dependence of the emission probability $P_2(p_1, x_A; p_2, x_B)$.

It may be useful to compare the physically motivated Kopylov-Podgoretsky approach with a more formal one based on Wigner functions [6] or space-time density matrix [7]. Thus, inserting the Fourier transform (4) into Eq. (1) and introducing the space-time density matrix

$$\rho_2(x_1, x_2; x_1', x_2') = \sum_{\{\alpha\}} \tilde{T}(x_1, x_2; \{\alpha\}) \tilde{T}^*(x_1', x_2'; \{\alpha\}) \tag{16}$$

and the notations: $\hat{x}_i = \frac{1}{2}(x_i + x_i')$, $\delta_i = x_i - x_i'$, $i = 1, 2$, and $\hat{x}_{12} = \hat{x}_1 - \hat{x}_2$, we can rewrite the production probability as

$$\begin{aligned} P_2^c(\mathbf{p}_1, \mathbf{p}_2) = \tfrac{1}{2!} \int [&\exp(ip_1\delta_1 + ip_2\delta_2) + \exp(ip_2\delta_1 + ip_1\delta_2) + 2\exp(ip_{12}(\delta_1 + \delta_2)) \cdot \\ &\cdot \cos(q_{12}\hat{x}_{12})] \rho_2(x_1, x_2; x_1', x_2') d^4x_1 d^4x_2 d^4x_1' d^4x_2'. \end{aligned} \tag{17}$$

Changing the integration variables: $x_i, x_i' \to \hat{x}_i, \delta_i$ and introducing the emission function as a partial Fourier transform of the space-time density matrix (an analog of the Wigner density):

$$\begin{aligned} &D_2(p, \hat{x}_1; p', \hat{x}_2) = \\ &= \int d^4\delta_1 d^4\delta_2 \exp(ip\delta_1 + ip'\delta_2) \rho_2(\hat{x}_1 + \tfrac{1}{2}\delta_1, \hat{x}_2 + \tfrac{1}{2}\delta_2; \hat{x}_1 - \tfrac{1}{2}\delta_1, \hat{x}_2 - \tfrac{1}{2}\delta_2), \end{aligned} \tag{18}$$

which is normalized in the same way as the function $P_2(p_1, x_A; p_2, x_B)$ (see Eq. (14)), we finally get

$$P_2^c(\mathbf{p}_1, \mathbf{p}_2) = \int d^4\hat{x}_1 d^4\hat{x}_2 [D_2(p_1, \hat{x}_1; p_2, \hat{x}_2) + D_2(p_{12}, \hat{x}_1; p_{12}, \hat{x}_2) \cos(q_{12}\hat{x}_{12})], \tag{19}$$

where $p_{12} = \frac{1}{2}(p_1 + p_2)$. The production probability in the case of no BE effect is given by the first term in Eq. (19):

$$P_2(\mathbf{p}_1, \mathbf{p}_2) = \int d^4\hat{x}_1 d^4\hat{x}_2 D_2(p_1, \hat{x}_1; p_2, \hat{x}_2). \tag{20}$$

Note that the result of Pratt [6] follows from Eq. (19) in the case of independent production of the two particles (see also the discussion in [8]) when

$$D_2(p_1, \hat{x}_1; p_2, \hat{x}_2) = D(p_1, \hat{x}_1) D(p_2, \hat{x}_2). \tag{21}$$

Making the *smoothness* assumption, i.e.

$$D_2(p_1, \hat{x}_1; p_2, \hat{x}_2) \doteq D_2(p_{12}, \hat{x}_1; p_{12}, \hat{x}_2), \tag{22}$$

and identifying the emission function D_2 with the emission probability P_2, we recover the Kopylov-Podgoretsky result in Eq. (12). This result can be also obtained directly from Eq. (17) if the *smoothness* condition was introduced on the level of the space-time density matrix as the requirement of a small width of its diagonal, determined by $\langle | \delta_i | \rangle$, compared with the characteristic space-time distance between particle production points, determined by $\langle | \hat{x}_1 - \hat{x}_2 | \rangle$ [7].

It may be useful to express the function D_2 through the Kopylov-Podgoretsky amplitudes $t(p_1, p_2; \{\alpha\})$ continued off mass-shell. Substituting Eq. (5) into Eq. (16) and using the inverted Fourier transform in Eq. (6), we get from Eq. (18):

$$D_2(p, \hat{x}_1; p', \hat{x}_2) = \frac{1}{(2\pi)^8} \sum_{\{\alpha'\}} \int d^4x_A d^4x_B d^4\kappa d^4\kappa' \exp(i\kappa(x_A - \hat{x}_1) + i\kappa'(x_B - \hat{x}_2)) \cdot$$
$$\cdot t(p + \tfrac{1}{2}\kappa, p' + \tfrac{1}{2}\kappa'; \{x_A, x_B, \alpha'\}) t^*(p - \tfrac{1}{2}\kappa, p' - \tfrac{1}{2}\kappa'; \{x_A, x_B, \alpha'\}). \tag{23}$$

Comparing Eqs. (13) and (23), we can see that the emission function D_2 is more spread in space and time than the emission probability P_2. In particular, assuming factorization of the production amplitude and its Gaussian parametrization (see Eqs. (8) and (9)) and similar Gaussian space-time distribution of the sources with spatial and time dispersions r_0^2 and τ_0^2, we get for the corresponding one-particle emission functions:

$$P(p, x) \sim \exp(-r_A^2 \mathbf{p}^2 - \tau_A^2 p_0^2) \exp(-\frac{\mathbf{x}^2}{2r_0^2} - \frac{x_0^2}{2\tau_0^2}) \tag{24}$$

and

$$D(p, x) \sim \exp(-r_A^2 \mathbf{p}^2 - \tau_A^2 p_0^2) \exp(-\frac{\mathbf{x}^2}{2r_0^2 + r_A^2} - \frac{x_0^2}{2\tau_0^2 + \tau_A^2}). \tag{25}$$

We should stress here, that the two approaches are equivalent in the sense, that both are based on Eqs. (1) and (4), and give the same result for the observables p_1 and p_2, using, however, parameterizations in terms of different space-time variables, $\hat{x}_1, \hat{x}_2$ and x_A, x_B, related by Eq. (23).

Concerning the connection with transport models, a question may arise about the meaning of the space-time coordinates of the particle production points calculated within these models. Considering, e.g., resonance or string decays or secondary interactions, it seems natural to identify these coordinates with those of the source centers and not with the ones of particle emission points in the Wigner sense. On the other hand, the exact result of Kopylov-Podgoretsky model (Eq. (11)) is formulated in terms of the production amplitudes, while in a classical transport model we have to deal with probabilities. From this point of view, the Wigner function formalism may seem to be more suitable provided that the final source sizes are taken into account in the transport model. But the problem is still there as the emission functions D_2, though being real, are not positively defined. Besides, the emission function $D_2(p_{12}, \hat{x}_1; p_{12}, \hat{x}_2)$ corresponds to off-mass-shell bosons with $p_{12}^2 \equiv \frac{1}{4}m_{12}^2 = m^2 - \frac{1}{4}q^2$, where m is the boson mass, and cannot be calculated in principle from a classical simulation. In case when the *smoothness* condition is valid these problems are avoided and the difference between the two approaches, due to the parametrizations in different space-time variables, disappears.

Let us define the correlation function as the ratio of the production probabilities with the effect of BE statistics switched on and switched off:

$$C_2(\mathbf{p}_1, \mathbf{p}_2) = P_2^c(\mathbf{p}_1, \mathbf{p}_2)/P_2(\mathbf{p}_1, \mathbf{p}_2). \tag{26}$$

Note that, in experiment, the reference probability $P_2(\mathbf{p}_1, \mathbf{p}_2)$ in the denominator of Eq. (26) is usually constructed with the help of particles from different events of similar type, neglecting possible dynamical correlations.

Inserting Eqs. (19) and (20) into Eq. (26), we obtain

$$C_2(\mathbf{p}_1,\mathbf{p}_2) = \frac{\int d^4x_1 d^4x_2 [D_2(p_1,x_1;p_2,x_2) + D_2(p_{12},x_1;p_{12},x_2)\cos(q_{12}x_{12})]}{\int d^4x_1 d^4x_2 D_2(p_1,x_1;p_2,x_2)}. \quad (27)$$

Under the *smoothness* assumption in Eq. (22), we can also use the approximate equation:

$$C_2(\mathbf{p}_1,\mathbf{p}_2) \doteq \frac{\int d^4x_1 d^4x_2 D_2(p_1,x_1;p_2,x_2)[1+\cos(q_{12}x_{12})]}{\int d^4x_1 d^4x_2 D_2(p_1,x_1;p_2,x_2)}. \quad (28)$$

In the case of independent production of the particles, when Eq. (21) is valid, we can write the correlation function in the form

$$C_2(\mathbf{p}_1,\mathbf{p}_2) = 1 + \mid F_{12} \mid^2, \quad (29)$$

where

$$F_{12} \equiv F(p_{12},q_{12}) = \frac{\int d^4x D(p_{12},x)\exp(iq_{12}x)}{[\int d^4x_1 D(p_1,x_1)\int d^4x_2 D(p_2,x_2)]^{\frac{1}{2}}}. \quad (30)$$

If the *smoothness* condition is valid, we can substitute the momenta p_1 and p_2 in the arguments of the emission functions by the mean 4-momentum p_{12} and write

$$F_{12} \doteq \frac{\int d^4x D(p_{12},x)\exp(iq_{12}x)}{\int d^4x D(p_{12},x)}. \quad (31)$$

We should stress that, generally, the factorization assumption in Eq. (21) is not necessary for the implementation of the two-particle BE correlations in transport models. Moreover, these models can contain additional dynamical correlations which would be lost in the case of such an assumption. However, for practical reasons, we will neglect the possible, but usually rather small, dynamical correlations in a transport model and assume the factorization when calculating the higher order correlations.

Besides the 6-dimensional correlation function defined in Eq. (26), we introduce the correlation function integrated over some of the kinematic variables characterizing the two-particle system. For example, the one-dimensional correlation function in terms of the variable $q_{inv} = \sqrt{-q_{12}^2} = \sqrt{m_{12}^2 - 4m^2}$ is defined as

$$C_2(q_{inv}) = \frac{\int \frac{d^3\mathbf{p}_1}{E_1}\frac{d^3\mathbf{p}_2}{E_2}\delta(q_{inv}-\sqrt{-q_{12}^2})P_2^c(\mathbf{p}_1,\mathbf{p}_2)}{\int \frac{d^3\mathbf{p}_1}{E_1}\frac{d^3\mathbf{p}_2}{E_2}\delta(q_{inv}-\sqrt{-q_{12}^2})P_2(\mathbf{p}_1,\mathbf{p}_2)}. \quad (32)$$

For practical calculations based on the event simulation within a transport model, it is convenient to introduce the non-invariant two-particle emission function

$$\tilde{D}_2(p_1,x_1;p_2,x_2) = \frac{1}{E_1E_2}D_2(p_1,x_1;p_2,x_2) \quad (33)$$

and production probability

$$\tilde{P}_2(p_1,p_2) = \int \tilde{D}_2(p_1,x_1;p_2,x_2)d^4x_1d^4x_2, \quad (34)$$

normalized by the conditions

$$\int d^3\mathbf{p}_1 d^3\mathbf{p}_2 d^4x_1 d^4x_2 \tilde{D}_2(p_1, x_1; p_2, x_2) = \int \tilde{P}_2(\mathbf{p}_1, \mathbf{p}_2) d^3\mathbf{p}_1 d^3\mathbf{p}_2 = 1. \tag{35}$$

Similarly, the non-invariant single-particle emission function

$$\tilde{D}(p, x) = \frac{1}{E} D(p, x) \tag{36}$$

and production probability

$$\tilde{P}(\mathbf{p}) = \int \tilde{D}(p, x) d^4x \tag{37}$$

are normalized by the conditions

$$\int d^3\mathbf{p} d^4x \tilde{D}(p, x) = \int \tilde{P}(p) d^3\mathbf{p} = 1. \tag{38}$$

It is clear that Eqs. (26)-(32) are valid also with the invariant functions substituted by the non-invariant ones and $\frac{d^3\mathbf{p}_i}{E_i} \to d^3\mathbf{p}_i$.

3 Two-boson correlation function: calculations

Generating events within a transport model as a set of phase-space points $\{k_i; r_i\} \equiv \{\omega_i, \vec{k}_i; t_i, \vec{r}_i\}$ of emitted bosons at their freeze-out times t_i, we can express the non-invariant single-particle emission function as

$$\tilde{D}(p, x) = \frac{1}{N} \sum_{i=1}^{N} \delta^3(\mathbf{p} - \mathbf{k}_i(r_i)) \delta^4(x - r_i) \equiv \left\langle \delta^3(\mathbf{p} - \mathbf{k}_i(r_i)) \delta^4(x - r_i) \right\rangle, \tag{39}$$

where $\omega_i = \sqrt{\mathbf{k}_i^2 + m^2}$ is the boson energy and N is total number of the simulated phase-space points. Usually dynamical models contain a correlation between space-time and momentum, which is denoted as $\mathbf{k}_i(r_i)$. The invariant emission function $D(p, x)$ is given by

$$D(p, x) = \left\langle \omega_i \delta^3(\mathbf{p} - \mathbf{k}_i(r_i)) \delta^4(x - r_i) \right\rangle = \left\langle \delta^2(\mathbf{p}_t - \mathbf{k}_{ti}(r_i)) \delta(y - y_i) \delta^4(x - r_i) \right\rangle, \tag{40}$$

where $\mathbf{p}_t$ and y are the boson transverse momentum and rapidity, respectively. One can see that these functions are properly normalized to unity. For some purposes it may be useful to construct the emission function in the momentum bins of a finite width $\Delta\mathbf{p}$. For example,

$$\tilde{D}(p, x) = \frac{1}{N} \int_{\mathbf{p}-\Delta\mathbf{p}/2}^{\mathbf{p}+\Delta\mathbf{p}/2} \frac{d^3\mathbf{p}'}{\Delta^3\mathbf{p}} \sum_{i=1}^{N} \delta^3(\mathbf{p}' - \mathbf{k}_i(r_i)) \delta^4(x - r_i) = \frac{1}{N\Delta^3\mathbf{p}} \sum_{l=1}^{\Delta N(\mathbf{p})} \delta^4(x - r_{i_l}), \tag{41}$$

where $\Delta^3\mathbf{p} = \Delta p_x \Delta p_y \Delta p_z$ and the number of contributing points $\Delta N(\mathbf{p})$ is determined by the condition:

$$\mathbf{k}_{i_l} \in \{\mathbf{p} - \Delta\mathbf{p}/2, \mathbf{p} + \Delta\mathbf{p}/2\}\,. \tag{42}$$

Eq. (41) can be also written in a more compact form:

$$\tilde{D}(p,x) = \frac{\Delta N(\mathbf{p})}{N\Delta^3\mathbf{p}} \left\langle \delta^4(x - r_i) \right\rangle_{\mathbf{p}}, \tag{43}$$

where $\langle ... \rangle_{\mathbf{p}}$ denotes the averaging over the phase-space points satisfying the condition (42). For the non-invariant single-particle production probability defined in Eq. (37), we get from Eqs. (39) or (43)

$$\tilde{P}(\mathbf{p}) = \frac{1}{N} \sum_{i=1}^{N} \delta^3(\mathbf{p} - \mathbf{k}_i(r_i)) \tag{44}$$

or

$$\tilde{P}(\mathbf{p}) = \frac{\Delta N(\mathbf{p})}{N\Delta^3\mathbf{p}}, \tag{45}$$

respectively.

Similarly, we can express the two-particle emission function and production probability obtained from a dynamical model. Thus the non-invariant emission function is given by

$$\begin{aligned}\tilde{D}_2(p_1,x_1;p_2,x_2) &= \tfrac{1}{M}\textstyle\sum_{l=1}^{M} \delta^3(\mathbf{p}_1 - \mathbf{k}_{i_l}(r_{i_l}))\delta^4(x_1 - r_{i_l})\delta^3(\mathbf{p}_2 - \mathbf{k}_{j_l}(r_{j_l}))\delta^4(x_2 - r_{j_l}) \equiv \\ &\equiv \langle \delta^3(\mathbf{p}_1 - \mathbf{k}_{i_l}(r_{i_l}))\delta^4(x_1 - r_{i_l})\delta^3(\mathbf{p}_2 - \mathbf{k}_{j_l}(r_{j_l}))\delta^4(x_2 - r_{j_l})\rangle\,,\end{aligned} \tag{46}$$

where $M = \frac{1}{2}N(N-1)$ is the total number of simulated pairs. In finite bins of $\mathbf{p}_1$, $\mathbf{p}_2$ one has

$$\begin{aligned}\tilde{D}_2(p_1,x_1;p_2,x_2) &= \tfrac{1}{M(\Delta^3\mathbf{p})^2}\textstyle\sum_{l=1}^{\Delta M(\mathbf{p}_1,\mathbf{p}_2)} \delta^4(x_1 - r_{i_l})\delta^4(x_2 - r_{j_l}) \equiv \\ &\equiv \tfrac{\Delta M(\mathbf{p}_1,\mathbf{p}_2)}{M(\Delta^3\mathbf{p})^2} \langle \delta^4(x_1 - r_{i_l})\delta^4(x_2 - r_{j_l})\rangle_{\mathbf{p}_1,\mathbf{p}_2}\,,\end{aligned} \tag{47}$$

where $\Delta M(\mathbf{p}_1,\mathbf{p}_2)$ is the number of pairs in given bin of $\mathbf{p}_1$, $\mathbf{p}_2$, i.e. satisfying the conditions

$$\begin{aligned}\mathbf{k}_{i_l} &\in \{\mathbf{p}_1 - \Delta\mathbf{p}/2, \mathbf{p}_1 + \Delta\mathbf{p}/2\}\,, \\ \mathbf{k}_{j_l} &\in \{\mathbf{p}_2 - \Delta\mathbf{p}/2, \mathbf{p}_2 + \Delta\mathbf{p}/2\}\,.\end{aligned} \tag{48}$$

The corresponding non-invariant two-particle production probabilities are

$$\tilde{P}_2(\mathbf{p}_1,\mathbf{p}_2) = \frac{1}{M} \sum_{l=1}^{M} \delta^3(\mathbf{p}_1 - \mathbf{k}_{i_l})\delta^3(\mathbf{p}_2 - \mathbf{k}_{j_l}) \tag{49}$$

or

$$\tilde{P}_2(\mathbf{p}_1,\mathbf{p}_2) = \frac{\Delta M(\mathbf{p}_1,\mathbf{p}_2)}{M(\Delta^3\mathbf{p})^2}. \tag{50}$$

Similarly, using Eq. (28), we can calculate the two-particle correlation function in finite bins of $\mathbf{p}_1$ and $\mathbf{p}_2$ as

$$C_2(\mathbf{p}_1, \mathbf{p}_2) = 1 + \langle \cos[(k_{i_l} - k_{j_l})(r_{i_l} - r_{j_l})] \rangle_{\mathbf{p}_1, \mathbf{p}_2} , \tag{51}$$

where $\langle ... \rangle_{\mathbf{p}_1, \mathbf{p}_2}$ is defined in Eq. (47). For the one-dimensional correlation function in Eq. (32), we get

$$C_2(q_{inv}) = 1 + \frac{1}{\Delta N(q_{inv})} \sum_{l=1}^{\Delta N(q_{inv})} \cos[(k_{i_l} - k_{j_l})(r_{i_l} - r_{j_l})], \tag{52}$$

where $\Delta N(q_{inv})$ is the number of the simulated pairs in a given bin of $q_{inv} = \sqrt{-q_{ij}^2}$.

We can also calculate the two-particle correlation function approximately, using Eq. (29) valid in the case of factorization of the two-particle emission function. For this we have to precompute the function F_{ij} according to Eq. (31). Using Eq. (41) for the emission function, we get

$$F_{ij} = \langle \exp(i q_{ij} r_{k_l}) \rangle_{\mathbf{p}_{ij}} . \tag{53}$$

Note that F_{ij} would become a function of q_{ij} only if the correlation between space-time and momentum were neglected. In this case, to obtain F_{ij}, we could average over all space-time points obtained from a transport model:

$$F_{ij} = \langle \exp(i q_{ij} r_k) \rangle . \tag{54}$$

In the interferometry context, Eq. (54) means that the whole space-time production region is 'visible'. To take into account the $x - p$ correlation, in practical calculations according to Eq. (53) it is suitable to introduce the bin in $\mathbf{p}_{ij}$ in terms of rapidity $y_{ij} = \frac{1}{2}(y_i + y_j)$ and transverse momentum $\mathbf{p}_{tij} = \frac{1}{2}(\mathbf{p}_{ti} + \mathbf{p}_{tj})$. The corresponding widths Δy and $\Delta \mathbf{p}_t$ can be found empirically by choosing sufficiently large starting values and then decreasing them till the function F_{ij} saturates.

We performed the classical simulation of the phase-space coordinates $\{k_i, r_i\}$ of emitted particles within the parton-string model [5]. This model is found to describe the global characteristics of ultra-relativistic hadron-hadron and nucleus-nucleus collisions reasonably well. To minimize the effect of final state interaction, we first considered neutral pions. To stress that the model contains a correlation between space-time and momentum, we plot in Fig. 2 the space-time rapidity $\eta = \frac{1}{2}\, ln \left(\frac{t+z}{t-z}\right)$ versus the momentum rapidity $y = \frac{1}{2} \ln \left(\frac{E+P_z}{E-P_z}\right)$ of the pions emitted in central (at zero impact parameter) $O + O$ collisions at initial energy $E_{lab} = 200$ AGeV.

In Fig. 3, we present the one-dimensional correlation functions calculated for central $O + O$ and $S + S$ collisions at initial energy $E_{lab} = 200$ AGeV. We have calculated two-pion correlation functions using several following options:

1) as usual for interferometry analysis within a transport model [4], we use Eq. (52) (the open triangles);

2) same as 1), but we choose space-time coordinates randomly to destroy the $x - p$ correlation in a given event (the full triangles);

3) we use the approximate Eq. (29), neglecting possible dynamical correlations in our particular model, and calculate F_{12} according to Eq. (53), taking into account the $x-p$ correlation (the open circles);

4) same as 3), but we calculate F_{12} according to Eq. (54), neglecting the $x-p$ correlation (the full circles).

It can be seen from Fig. 3 that the $x-p$ correlation, presented in the model, influences the two-pion correlation function in correspondence with a decrease of the effective space-time distance between the particle production points. Coincidence of the results 1) and 3) indicates that we can neglect dynamical correlations and use F_{ij} values, precomputed according to Eq. (53), for calculation of the higher order BE correlations (see Section 4).

Substituting Eq. (29) into the relation

$$P_2^c(\mathbf{p}_1,\mathbf{p}_2) = P(\mathbf{p}_1)P(\mathbf{p}_2)C_2(\mathbf{p}_1,\mathbf{p}_2), \tag{55}$$

valid in the case of negligible dynamical correlations, and performing integration (summation in our model) over the momentum $\mathbf{p}_2$ of the second particle, we get the invariant single-particle production probability containing the two-particle BE effect (see also [9] and [10]):

$$P_2^c(\mathbf{p}_1) = \frac{P(\mathbf{p}_1)}{(1+K_2)}[1+K_2(\mathbf{p}_1)], \tag{56}$$

where

$$K_2(\mathbf{p}_1) = \left\langle \mid F_{i_1 j_1} \mid^2 \right\rangle_{\mathbf{p}_1} \tag{57}$$

and

$$K_2 = \left\langle \mid F_{i_1 j_1} \mid^2 \right\rangle. \tag{58}$$

Note that here the invariant production probability $P_2^c(\mathbf{p}_1)$ is normalized to unity as $\int \frac{d^3\mathbf{p}_1}{E_1} P_2^c(\mathbf{p}_1) = 1$. For the non-invariant probability $\tilde{P}_2(\mathbf{p}_1)$ holds the relation similar to Eq. (56), but with the normalization condition $\int d^3\mathbf{p}_1 \tilde{P}_2^c(\mathbf{p}_1) = 1$.

It follows from our calculations based on the particular model of the ultra-relativistic nucleus-nucleus collisions [5], that the two-particle BE correction to the single-particle production probability (expressed by Eq. (56)) is practically negligible.

4 Higher order correlation functions

Let us first consider the events with $n = 3$ identical spinless bosons. Assuming uncorrelated emission and absence of final state interaction, but taking into account the requirements of BE statistics, we get the three-particle invariant production proba-

bility

$$
\begin{aligned}
P_3^c(\mathbf{p}_1,\mathbf{p}_2,\mathbf{p}_3) = \int d^4x_1 d^4x_2 d^4x_3 [&D(p_1,x_1)D(p_2,x_2)D(p_3,x_3)+ \\
&+D(p_3,x_3)D(p_{12},x_1)D(p_{12},x_2)\cos(q_{12}x_{12})+ \\
&+D(p_2,x_2)D(p_{13},x_1)D(p_{13},x_3)\cos(q_{13}x_{13})+ \\
&+D(p_1,x_1)D(p_{23},x_2)D(p_{23},x_3)\cos(q_{23}x_{23})+ \\
&+2D(p_{12},x_1)D(p_{23},x_2)D(p_{13},x_3)\cos(q_{12}x_1+q_{23}x_2+q_{31}x_3)].
\end{aligned}
\tag{59}
$$

In the case of switched off the effect of BE statistics, this probability becomes

$$
P_3(\mathbf{p}_1,\mathbf{p}_2,\mathbf{p}_3) = \int d^4x_1 d^4x_2 d^4x_3 D(p_1,x_1)D(p_2,x_2)D(p_3,x_3). \tag{60}
$$

From a classical simulation, neglecting rather small dynamical correlations, it can be calculated as

$$
P_3(\mathbf{p}_1,\mathbf{p}_2,\mathbf{p}_3) \doteq P(\mathbf{p}_1)P(\mathbf{p}_2)P(\mathbf{p}_3), \tag{61}
$$

where $P(\mathbf{p}_i) = E_i\tilde{P}(\mathbf{p}_i)$ can be computed from Eq. (44). Similarly to the two-particle case we define three-particle correlation function in the events with three identical particles as

$$
C_3(\mathbf{p}_1,\mathbf{p}_2,\mathbf{p}_3) = \frac{P_3^c(\mathbf{p}_1,\mathbf{p}_2,\mathbf{p}_3)}{P_3(\mathbf{p}_1,\mathbf{p}_2,\mathbf{p}_3)}. \tag{62}
$$

Inserting Eqs. (59) and (61) into Eq. (62) and using the *smoothness* assumption, we can write the correlation function in terms of the function F_{ij} as (see, e.g., [3])

$$
C_3(\mathbf{p}_1,\mathbf{p}_2,\mathbf{p}_3) = 1 + |F_{12}|^2 + |F_{23}|^2 + |F_{31}|^2 + 2Re\{F_{12}F_{23}F_{31}\}. \tag{63}
$$

Like in the two-particle case, from a classical simulation we can calculate the dependence of the three-particle correlation function on the invariant variable $q_{inv} = \sqrt{-q_{123}^2} = \sqrt{m_{123}^2 - 9m^2}$, where m_{123} is the effective mass of the system of three identical particles of mass m, as

$$
C_3(q_{inv}) = \frac{1}{N(q_{inv})}\sum_{i=1}^{N(q_{inv})} C_3(\mathbf{p}_{1_i},\mathbf{p}_{2_i},\mathbf{p}_{3_i}). \tag{64}
$$

Here $N(q_{inv})$ is the number of particle triplets in a given q_{inv} bin and $C_3(\mathbf{p}_{1_i},\mathbf{p}_{2_i},\mathbf{p}_{3_i})$ is defined by expression (63). In Fig. 4, we show the pure (only the last term in Eq. (63)) three-pion correlation functions for central $O+O$ and $S+S$ collisions simulated according to the parton-string model [5] at $E_{lab} = 200$ AGeV with F_{ij} calculated according to Eq. (53).

We note that the last term in Eq. (63) is sensitive to the phases of F_{ij} provided the emission function has no center of symmetry in 4-coordinate space. Thus, the measurement of the correlation functions of three or more identical bosons, besides the consistency check of the results of the two-particle interferometry, can give, in principle, an information about the asymmetry of the space-time distribution of the emission points [11].

Using Eqs. (61)-(63) and performing integration over the momenta of two or one of the three identical particles, we obtain the following expressions for the normalized

invariant single-particle production probability:

$$P_3^c(\mathbf{p}_1) = \frac{P(\mathbf{p}_1)}{(1+3K_2+K_3)}[1+2K_2(\mathbf{p}_1)+K_2+K_3(\mathbf{p}_1)] \tag{65}$$

and the two-particle correlation function:

$$C_3(\mathbf{p}_1,\mathbf{p}_2) = 1+|F_{12}|^2+K_2(\mathbf{p}_1)+K_2(\mathbf{p}_2)+K_3(\mathbf{p}_1,\mathbf{p}_2), \tag{66}$$

where

$$K_3(\mathbf{p}_1,\mathbf{p}_2) = \langle 2Re\{F_{i_lj_l}F_{j_lk_l}F_{k_li_l}\}\rangle_{\mathbf{p}_1,\mathbf{p}_2}, \tag{67}$$

$$K_3(\mathbf{p}_1) = \langle 2Re\{F_{i_lj_l}F_{j_lk_l}F_{k_li_l}\}\rangle_{\mathbf{p}_1} \tag{68}$$

and

$$K_3 = \langle 2Re\{F_{i_lj_l}F_{j_lk_l}F_{k_li_l}\}\rangle\,. \tag{69}$$

One can find similar formulae in paper [10] for the special case of Gaussian emission function.

The extension of these considerations to the events with larger number of produced particles is straightforward. For example, in the case of independent production of four identical spinless particles, the four-particle correlation function can be written in terms of F_{ij} as

$$\begin{aligned} C_4(\mathbf{p}_1,\mathbf{p}_2,\mathbf{p}_3,\mathbf{p}_4) = 1 + \sum_{\alpha(i<j)=1}^{6}|F_{ij}|^2 + \sum_{\alpha(1\neq j\neq k\neq l)=1}^{3}|F_{1j}|^2\,|F_{kl}|^2 + \\ + \sum_{\alpha(i<j<k)=1}^{4} 2Re\,\{F_{ij}F_{jk}F_{ki}\} + \sum_{\alpha(1\neq j\neq k\neq l)=1}^{3} 2Re\,\{F_{1j}F_{jk}F_{kl}F_{l1}\}\,, \end{aligned} \tag{70}$$

where α numerate combinations or odd permutations of the elements of the sequence $\{1,2,3,4\}$. Using the relation analogous to Eq. (55), we can compute the BE corrections for single-particle spectra and two-particle correlation functions due to the presence of additional identical bosons similarly as in the two- and three-particle cases.

Finally, we can define the n-particle correlation function in the events with n identical spinless particles as a ratio of the invariant production probability $P_n^c(\mathbf{p}_1,\mathbf{p}_2,...,\mathbf{p}_n)$ including the effect of BE symmetrization to the one, $P(\mathbf{p}_1,\mathbf{p}_2,...,\mathbf{p}_n)$, obtained from a classical simulation:

$$C_n(\mathbf{p}_1,\mathbf{p}_2,...\mathbf{p}_n) = P_n^c(\mathbf{p}_1,\mathbf{p}_2,...,\mathbf{p}_n)/P_n(\mathbf{p}_1,\mathbf{p}_2,...,\mathbf{p}_n). \tag{71}$$

Neglecting dynamical correlations and putting

$$P_n(\mathbf{p}_1,\mathbf{p}_2,...,\mathbf{p}_n) = \prod_{i=1}^{n} P(\mathbf{p}_i), \tag{72}$$

we can express the correlation function in terms of F_{ij} as (see also [10, 12])

$$C_n(\mathbf{p}_1,\mathbf{p}_2,...,\mathbf{p}_n) = \sum_{\sigma}\prod_{i=1}^{n} F_{i\sigma_i}. \tag{73}$$

The sum in Eq. (73) is over $n!$ possible permutations σ of the sequence $\{1, 2, 3, ..., n\}$.

As one can see from Eqs. (63) and (70), the higher order correlation functions consist mainly of the statistical combinations of the lower order correlations. The genuine higher order correlations are measured by the so-called particle cumulants. For example, the three-particle cumulant

$$K_3(\mathbf{p}_1, \mathbf{p}_2, \mathbf{p}_3) = 2Re\{F_{12}F_{23}F_{31}\} \tag{74}$$

in Eq. (63) or the four-particle cumulant

$$K_4(\mathbf{p}_1, \mathbf{p}_2, \mathbf{p}_3, \mathbf{p}_4) = \sum_{\alpha(1\neq j\neq k\neq l)=1}^{3} 2Re\{F_{1j}F_{jk}F_{kl}F_{l1}\} \tag{75}$$

in Eq. (70) measure the statistical dependence of the whole 3- or 4-particle set. Any of the three or four particles is independent of the others if the corresponding cumulant is zero. From a classical simulation, we are able to calculate the three- and four-particle cumulants from Eqs. (53), (74) and (75) and compare them with the existing experimental data to test the model. These cumulants calculated for high energy nucleus-nucleus collisions within our particular dynamical model [5] appear to be clearly non-zero for neutral pions (see, e.g., Fig. 4), while for charged ones they are strongly damped by the Coulomb repulsion effects (see Fig. 8 and discussion in Section 6). Note that substantially non-zero cumulants of identical charged pions would be in contradiction with the results of intermittency analysis of high energy experimental data [13]. In this analysis, the cumulants of the order three or higher are found non-zero in hadron-hadron or e^+e^- interactions, while for nucleus-nucleus collisions they appear to be practically vanishing.

5 Higher order BE corrections

As one can see from formulae (56), (65) and (66), the two- and three-particle BE correlations lead to distortions of the original single- and two-particle distributions. Such distortions are small in the case of interference of only two or three identical particles. However, as it was pointed out in paper [10] (see also [3] and [15]), they can become essential for the events with a large number of identical spinless particles due to factorially increasing number of correction terms.

To account for the multi-boson symmetrization effect, in papers [10, 14] a phase-space weighting procedure was used with weights in the form of a normalized square of the sum of $n!$ plane waves, like that in Eq. (15) for the case $n = 2$. This procedure however appears not practical for large numbers n of identical bosons due to the factorially large number of the terms to be computed to calculate the weight and, due to large weight fluctuations. These fluctuations can be substantially reduced by weighting only in the momentum space. The corresponding weights can be identified with the correlation functions $C_n(\mathbf{p}_1, \mathbf{p}_2, ..., \mathbf{p}_n)$ constructed from the precalculated

functions F_{ij} (see Eqs. (29), (63) and (70) for the cases $n = 2, 3$ and 4, respectively). However, there is still the problem with factorially large number of the terms required to calculate the weight according to Eq. (73).

A strong reduction of the number of calculated terms can be achieved by substituting the weight method by numerical integration, similarly to the considered two- or three-particle cases. We thus should perform integration over momenta of one or more particles in the inverted Eq. (71), i.e. we have to compute $K_2(\mathbf{p}_1)$, K_2, $K_3(\mathbf{p}_1, \mathbf{p}_2)$, $K_3(\mathbf{p}_1)$ and K_3, defined in Eqs. (57), (58), (67), (68) and (69), respectively, and corresponding average values of the higher order cumulants. We should also perform combinatorics to define multiples of these averaged cumulants. The last performance can be fulfilled up to all orders. Thus the statistical weight $\omega(n) = \int P_n^c(\mathbf{p}_1, \mathbf{p}_2, ..., \mathbf{p}_n) \prod_{i=1}^{n} \frac{d^3\mathbf{p}_i}{E_i}$ of an event with n identical spinless particles can be calculated with the help of the recurrence relation (see also [3, 15]):

$$\omega(n) = \sum_{j=0}^{n-1} C_j^{n-1} K_{j+1} \omega(n-j-1), \tag{76}$$

with C_j^{n-1} being the number of combinations of j elements out of $n-1$, $K_1 = 1$, $\omega(0) = \omega(1) = 1$ and $\omega(n) = 0$ for $n < 0$. One can check that $\omega(n) = n!$ in the case of 'coherent' particle emission (e.g., the emission from a very small space-time region) when $K_{j+1} = j!$.

However, for realistic models used to predict particle production in ultra-relativistic heavy-ion collisions, the numerical averaging of the cumulants of all orders is a difficult task. An attempt to take into account all the multi-particle interference pattern was recently considered by Pratt [16]. In this paper corrections to multiplicity distributions, single-particle spectra and two-particle correlation functions were calculated using the relativistic Bjorken model [17] for the emission function. To compute cumulants up to tenth order, the integration was performed analytically over the space-time coordinates and numerically over the momenta.

We should also mention the method of the correlation integral, developed by Carruthers and co-workers [18], based on a recursion expression of the integrated cumulants through the lower order ones. This method can be used as a tool for calculation of the integrated cumulants of arbitrary order.

As a first approximation, representing a lower estimate of the effect of Bose symmetrization, we neglect higher than the second order cumulants in Eq. (73). We will call it the second order cumulant approximation or simply the two-particle approximation. We recall that there is no experimental evidence for significantly nonzero values of the higher than second order cumulants in nucleus-nucleus collisions at high energies. In this approximation, we can express the statistical weight $\omega(n_i)$ of an event $i = 1, 2, ..., N_{evt}$ with n_i identical spinless particles in final state as

$$\omega(n_i) = 1 + \sum_{\alpha=1}^{n_i} D(n_i, \alpha) {K_2}^{\alpha}, \tag{77}$$

where $D(n_i, \alpha) = \frac{n_i!}{(n_i - 2\alpha)! \alpha! (2!)^{\alpha}}$. For practical calculations of this weight it is more

convenient to use the recurrence relation (76) reduced to:

$$\omega(n_i) = \omega(n_i - 1) + (n_i - 1)K_2\omega(n_i - 2). \tag{78}$$

It should be stressed that the account of the third or still higher order cumulants is straightforward and has to be done to check the convergence of such a lowest order cumulant expansion. A fast convergence is expected for the processes, such as heavy-ion collisions, characterized by a large space-time extent of the pion production region. In this paper, we limit ourselves to the second order cumulant approximation which appears to be sufficient for our purpose: to demonstrate a strong influence of the multi-particle BE effects.

The knowledge of the statistical weights for events with different number n of produced identical particles gives us a possibility to compute the effect of BE statistics on the multiplicity distribution

$$W(n) = \frac{1}{N_{evt}} \sum_{i=1}^{N_{evt}} \delta(n - n_i) \tag{79}$$

obtained in a classical simulation [15]. The BE corrected multiplicity distribution can be calculated as

$$W^c(n) = \sum_{i=1}^{N_{evt}} \delta(n - n_i)\omega(n_i) / \sum_{i=1}^{N_{evt}} \omega(n_i). \tag{80}$$

In the two-particle approximation, the normalized invariant single-particle probability for the events with n identical spinless bosons takes the form:

$$P_n^c(\mathbf{p}_1) = \frac{P(\mathbf{p}_1)}{\omega(n)}[\omega(n-1) + (n-1)K_2(\mathbf{p}_1)\omega(n-2)], \tag{81}$$

leading to Eq. (78) after the integration over the momentum $\mathbf{p}_1$. Note that Eq. (81) reduces to Eqs. (56) or (65) (with $K_3(\mathbf{p}_1) = K_3 = 0$) for $n = 2$ or $n = 3$, respectively.

For the two-particle correlation function in the events with n identical particles, we have in given approximation:

$$\begin{aligned} C_n(\mathbf{p}_1, \mathbf{p}_2) = \omega(n-2)(1 + |F_{12}|^2) + (n-2)\omega(n-3)(K_2(\mathbf{p}_1) + K_2(\mathbf{p}_2)) + \\ +(n-2)(n-3)\omega(n-4)K_2(\mathbf{p}_1)K_2(\mathbf{p}_2). \end{aligned} \tag{82}$$

One can check that Eq. (82) leads to Eq. (81) after multiplying it by $P(\mathbf{p}_2)$ and integrating over the momentum $\mathbf{p}_2$. For $n = 2$ or $n = 3$ Eq. (82) reduces to Eqs. (29) or (66) (without $K_3(\mathbf{p}_1, \mathbf{p}_2)$ term), respectively.

As expected, our calculations confirm that the effect of BE statistics for the events with a large number n of identical bosons leads to substantial distortions of the multiplicity distributions, the single-particle spectra and the two-boson correlation functions. This is demonstrated in Figs. 5-7 for central $O + O$ and $S + S$ collisions simulated within the parton-string model [5] at $E_{lab} = 200$ AGeV.

In Fig. 5 we show the original and BE corrected multiplicity distributions of neutral pions calculated from $N_{evt} = 20000$ generated events of $O+O$ collisions. As the

reconstruction of the tail of the BE corrected multiplicity distribution is practically impossible, we have fitted the simulated multiplicity distribution by a superposition of Poissonians (full curve) and used this fit to properly normalize the BE corrected points (dashed curve). A dramatic increase of the population of high multiplicities due to the effect of BE statistics ($K_2 = 0.0056$) is observed: the simulated mean multiplicity of 44.7 is increased by about 21 units.

In Fig. 6 we show the neutral pion transverse momentum distributions $\frac{1}{N}\frac{dN}{dp_t}$ and rapidity distributions $\frac{1}{N}\frac{dN}{dy}$ respectively obtained from the events generated with fixed neutral pion multiplicities $n = 30, 60$ in $O+O$ and $n = 100$ in $S+S$ collisions. In Fig. 6 we also draw the ratios of BE corrected and uncorrected single-particle distributions. We can see that the BE symmetrization enhances production of the pions with low p_t and small y, and that this effect becomes more pronounced with increasing pion multiplicity.

We should note here that in several papers (see, for example, review [3] and recent paper [15]) a possible enormous influence of BE statistics on the single-pion spectra and multiplicity distributions was argued and, in particular, the idea of pion laser, i.e. production of pions collimated in narrow and monochromatic jets, was discussed.

In Fig. 7 we present a ratio of the renormalized two-particle correlation functions $C_n(q_{inv})/\omega(n)$ and $C_2(q_{inv})/\omega(2)$ calculated for the events generated with fixed neutral pion multiplicities $n = 30$ and 60 in $O + O$ collisions. We can see that the multi-boson BE correlations distort the two-body correlation function in such a way that it becomes lower and wider. This is in qualitative agreement with the results of papers [10, 14, 15].

Concerning the two-pion interferometry, we note that the experimental correlation function is calculated as a ratio of the measured two-particle distribution to the reference one, the latter being usually also influenced by multi-pion BE correlations (the so-called residual correlations [10, 14]). For correct comparison of the theoretical and experimental correlation functions, in the case when the event mixing technique is used to construct the reference distribution, one has to take into account the change of the single-particle spectra according to Eq. (81).

So far we considered identical bosons as free particles and completely neglected their interaction. However, it is well-known (see, e.g., [19, 20]) that particle correlations at small relative velocities can be strongly affected by this interaction. Thus the effect of final state interaction is used as an important part of particle interferometry. Due to the unsolved multi-body interaction problem, usually, only the mutual interaction of two particles with a small relative velocity is taken into account, similar to the considered two-particle approximation (see next Section).

6 The effect of final state interactions

Let us now consider the production of interacting particles. As usual, we assume that the density of the produced particles in momentum space is sufficiently low so that

only the final state interaction in the pairs of particles with small relative velocities is to be taken into account. In the case of the production of only two identical spinless particles the effect of final state interaction then reduces to the substitution of the plane waves in Eq. (4) by the nonsymmetrized Bethe-Salpeter amplitudes $\Psi^{(+)}_{p_1p_2}(x_1,x_2)$ in the continuous spectrum of the two-particle states [7, 20]:

$$T(p_1,p_2;\{\alpha\}) = \int d^4x_1 d^4x_2 \Psi^{(+)}_{p_1p_2}(x_1,x_2)\tilde{T}(x_1,x_2;\{\alpha\}). \tag{83}$$

Under the *smoothness* assumption the two-particle production probability becomes

$$\begin{gathered} P^c_2(\mathbf{p}_1,\mathbf{p}_2) = \\ = \int d^4x_1 d^4x_2 D_2(p_1,x_1;p_2,x_2)\{\mid \Psi^{(+)}_{p_1p_2}(x_{12}) \mid^2 + Re[\Psi^{(+)}_{p_1p_2}(x_{12})\Psi^{(+)*}_{p_2p_1}(x_{12})]\}, \end{gathered} \tag{84}$$

where the amplitude $\Psi^{(+)}_{p_1p_2}(x_{12})$ is obtained from the Bethe-Salpeter amplitude after separation of the c.m.s. motion of the two particles:

$$\Psi^{(+)}_{p_1p_2}(x_1,x_2) = \exp(ip_{12}(x_1+x_2))\Psi^{(+)}_{p_1p_2}(x_{12}). \tag{85}$$

At equal emission times $t^*_1 = t^*_2$ in the two-particle c.m.s. the amplitude $\Psi^{(+)}_{p_1p_2}(x_{12})$ coincides with the wave function $\Psi^{(+)}_{-\mathbf{k}^*}(\mathbf{r}^*)$, $\mathbf{k}^* = \mathbf{p}^*_1 = -\mathbf{p}^*_2$, $\mathbf{r}^* = \mathbf{x}^*_{12}$, representing solution of the scattering problem and having the asymptotics of a superposition of the plane and outgoing spherical waves. It can be shown [20] that the amplitude $\Psi^{(+)}_{p_1p_2}(x_{12})$ can be usually substituted by this solution, leading to the *equal time* approximation first used by Koonin to calculate the correlation function of two non-relativistic protons [19].

In the case when three identical spinless particles are produced, on the assumption of saturation of the final state interaction by the two-body effects, the three-body nonsymmetrized Bethe-Salpeter amplitude can be approximated as

$$\Psi^{(+)}_{p_1p_2p_3}(x_1,x_2,x_3) \simeq \exp(ip_1x_1 + ip_2x_2 + ip_3x_3)\Phi_{12}(x_{12})\Phi_{31}(x_{31})\Phi_{23}(x_{23}), \tag{86}$$

where

$$\Phi_{ij}(x_{ij}) = \exp(-ip_ix_i - ip_jx_j)\Psi^{(+)}_{p_ip_j}(x_i,x_j) \equiv \exp(-\frac{1}{2}iq_{ij}x_{ij})\Psi^{(+)}_{p_ip_j}(x_{ij}). \tag{87}$$

Assuming now besides *smoothness* of the emission probability also its factorization, we get the following expression for the three-particle production probability:

$$\begin{gathered} P^c_3(\mathbf{p}_1,\mathbf{p}_2,\mathbf{p}_3) = \\ = \int d^4x_1 d^4x_2 d^4x_3 D(p_1,x_1)D(p_2,x_2)D(p_3,x_3) \mid \Psi^{(+)}_{p_1p_2}(x_{12})\Psi^{(+)}_{p_3p_1}(x_{31})\Psi^{(+)}_{p_2p_3}(x_{23}) \mid^2 \cdot \\ \cdot\{1 + \frac{Re[\Psi^{(+)}_{p_1p_2}(x_{12})\Psi^{(+)*}_{p_2p_1}(x_{12})]}{|\Psi^{(+)}_{p_1p_2}(x_{12})|^2} + \frac{Re[\Psi^{(+)}_{p_1p_3}(x_{13})\Psi^{(+)*}_{p_3p_1}(x_{13})]}{|\Psi^{(+)}_{p_1p_3}(x_{13})|^2} + \frac{Re[\Psi^{(+)}_{p_2p_3}(x_{23})\Psi^{(+)*}_{p_3p_2}(x_{23})]}{|\Psi^{(+)}_{p_2p_3}(x_{23})|^2} + \\ +2Re\exp(iq_{12}x_1 + iq_{31}x_3 + iq_{23}x_2)\}. \end{gathered} \tag{88}$$

The generalization of Eqs. (84) and (88) to the case of n identical spinless bosons is straightforward.

We define the n-particle correlation function, similar to the case of non-interacting bosons (see Eq. (71)), as a ratio of the production probability $P_n^c(\mathbf{p}_1,\mathbf{p}_2,...,\mathbf{p}_n)$, including both the effects of BE statistics and particle final state interaction, to that, $P_n(\mathbf{p}_1,\mathbf{p}_2,...,\mathbf{p}_n)$, obtained from a classical simulation. As one can see from Eqs. (84) and (88), the calculation of the n-particle correlation function requires to compute $n(n-1)$ amplitudes $\Psi^{(+)}_{p_ip_j}(x_{ij})$ and $\Psi^{(+)}_{p_jp_i}(x_{ij})$ for each event simulated in a transport model. Clearly, even on the factorization assumption, this calculation is much more complicated than in the case of pure BE correlations since the integration over space-time coordinates of n production points is not reduced to the single space-time point integration (like in Eq. (53)).

For neutral pions at small relative momenta $k^* = |\mathbf{k}^*| = \frac{1}{2}q_{inv}$, we are interested in, the scattered wave in the wave function $\Psi^{(+)}_{-\mathbf{k}^*}(\mathbf{r}^*)$ is dominated by s-wave. Since usually the characteristic distances r^* between the pion production points are larger than the range of their strong interaction, we can write

$$\Psi^{(+)}_{-\mathbf{k}^*}(\mathbf{r}^*) \doteq \exp(-i\mathbf{k}^*\mathbf{r}^*) + f(k^*)\frac{\exp(ik^*r^*)}{r^*}, \tag{89}$$

where $f(k^*)$ is the two-pion s-wave scattering amplitude. In such conditions, the effect of strong final state interaction on the correlation function is determined by the ratio of the scattering amplitude $f(k^*)$ to the characteristic distance between the production points in the c.m.s. of the two particles [20]. As the $\pi^0\pi^0$ scattering length is positive and rather small ($f(0) \simeq 0.1$ fm), the final state interaction slightly enhances (less than 5%) the effect of BE correlation in the system of two neutral pions.

For identical charged pions the effect of final state interaction is dominated by the Coulomb interaction. In the usual case, when the characteristic distance between particle production points in their c.m.s. is much smaller than the two-pion Bohr radius $a = 388$ fm, it can be approximated by the Coulomb penetration factor representing modulus squared of the Coulomb wave function at zero distance:

$$A_c(k^*) = \tfrac{2\pi}{ak^*}[\exp(\tfrac{2\pi}{ak^*}) - 1]^{-1}. \tag{90}$$

Thus, in given approximation, we have to multiply the pure BE n-particle correlation function by the product of $\frac{n(n-1)}{2}$ Coulomb penetration factors. For example, the three-particle correlation function in the events with three identical charged pions then takes the form:

$$C_3(\mathbf{p}_1,\mathbf{p}_2,\mathbf{p}_3) = A_c(k^*_{12})A_c(k^*_{13})A_c(k^*_{23})\tilde{C}_3(\mathbf{p}_1,\mathbf{p}_2,\mathbf{p}_3), \tag{91}$$

where $\tilde{C}_3(\mathbf{p}_1,\mathbf{p}_2,\mathbf{p}_3)$ is the correlation function in the absence of final state interaction, given by Eq. (63). It is clear from Eq. (90) that the Coulomb repulsion strongly suppresses the correlation of two identical charged pions only in the region of very small relative momenta $k^* < \frac{2\pi}{a} = 3$ MeV/c. Taking account of the relation

$$q_{inv}^{(123)2} = q_{inv}^{(12)2} + q_{inv}^{(13)2} + q_{inv}^{(23)2}, \tag{92}$$

this corresponds to the suppression of the three-particle correlation function in the region $q_{inv}^{(123)} < 6\sqrt{3}$ MeV/c. Thus the final state interaction in the system of identical charged pions becomes of increasing importance with increasing the effective space-time extent of the production region.

In Fig. 8, we show the two-particle (Eq. (29)) and the pure three-particle (only the last term in Eq. (63)) correlation functions of positively charged pions calculated with and without the Coulomb penetration factors for central $S + S$ collisions simulated within the parton-string model [5] at $E_{lab} = 200$ AGeV. It may be seen from Fig. 8 that the Coulomb effect in the system of three charged pions is quite strong even at $q_{inv}^{(123)}$ of several tens MeV/c. Thus the Coulomb repulsion may be responsible for the vanishing of the third and higher order cumulants of identical charged pions as measured in nucleus-nucleus collisions. The influence of the Coulomb final state interaction will be even stronger in future heavy ion experiments at higher energies due to increasing effective space-time extent of the particle production region.

Concerning the Coulomb effects in a multi-pion system, they should somewhat weaken the considered effects of the multi-particle BE correlations, depending on the effective space-time extent of the production region of charged pions. Though their detailed investigation is beyond the scope of present paper, it is certainly of a large practical interest. Here we only mention that such an investigation would require consideration of the pions of both signs (for $\pi^+\pi^-$ pairs there will be Coulomb attraction corresponding to the negative Bohr radius $a = -388$ fm in Eq. (90)) and, eventually, of other charged particles; the total production probability, in the absence of dynamical correlations, being just a product of the production probabilities of various particle species.

7 Conclusions

Large numbers of identical bosons are produced in ultra-relativistic heavy-ion collisions. Their production can be strongly affected by the requirements of quantum statistics. However, these requirements are usually neglected in classical simulations within transport models (event generators) which are widely used for description of the multi-particle production.

We have presented here the theoretical basis allowing to calculate the effect of the multi-particle BE correlations on various observables within a classical transport model. We have also discussed the inclusion of the effect of Coulomb and strong final state interaction in the produced multi-particle system.

We have developed the computer code BOSE which can be coupled with a classical transport model to account for the effects of BE statistics and final state interaction and thus to allow a reliable comparison of the model with experimental data. Coupling this code with the parton-string model, we have demonstrated the importance of the multi-particle BE effects on multiplicity distributions, single-pion spectra and two-pion correlation functions.

8 Acknowledgements

Enlightening discussions with Jörg Aichelin, Guy Paic and Jan Pluta are gratefully acknowledged. This work was possible due to the financial support of the Centre National de Recherches Scientifiques.

References

[1] G. Goldhaber *et. al.*, Phys. Rev. **120** (1960) 300.

[2] G. I. Kopylov and M. I. Podgoretsky, Sov. J. Nucl. Phys. **15** (1972) 219; ibid. **19** (1974) 215; G. I. Kopylov, Phys. Lett. **B50** (1974) 572.

[3] M. I. Podgoretsky, Sov. J. Part. Nucl., **20** (1989) 266; M. I. Podgoretsky, JINR Report **P2-85-240** (1985). SJPNP

[4] S. Pratt *et al.* in: Proc. of "Quark matter 94", Nucl. Phys. **A566** (1994) 103c.

[5] N. S. Amelin, M. Braun and C. Pajares, Z. Phys. **C63** (1994) 507; N. S. Amelin, H. Stöcker, W. Greiner, N. Armesto and C. Pajares, In: Proc. NATO Advanced Study Institute, eds. W. Greiner, H. Stöcker and A. Gallmann, Plenum Publishing, N. Y. (1994) 809.

[6] S. Pratt, Phys. Rev. Lett. **53** (1984) 1219; Phys. Rev. **D33** (1986) 1314.

[7] R. Lednicky, V. L. Lyuboshitz, in: Proc. Int. Workshop on Particle Correlations and Interferometry in Nuclear Collisions, CORINNE 90, **Nantes**, France (ed. D. Ardouin, World Scientific, 1990) p. 42; JINR Report **P2-546-92** (1992).

[8] G. F. Bertsch, P. Danielewich, M. Herrmann, INT Report **DOE/ER/40561-112-INT93-00-37** (1993).

[9] M. Gyulassy, S. Kauffman and L. Wilson, Phys. Rev. **C20** (1979) 2267; K. Kolehmainen and M. Gyulassy, Phys. Lett. **180B** (1986) 203.

[10] W. Zajc, Phys. Rev. **D35** (1987) 3396; W. Zajc *et al.*, Phys. Rev. **C29** (1984) 2173.

[11] V. L. Lyuboshitz, JINR Report **E2-90-361,** Dubna, 1990; In: Proc. of Int. Workshop on Correlations and Multiple Production (CAMP), **Marburg**, FRG, May 14-16, 1990, ed. R. Weiner, p. 114-123.

[12] S. S. Padula, M. Gyulassy and S. Gavin, Nucl. Phys. **B329** (1990) 357.

[13] P. Carruthers and I. Sarcevic, Phys. Rev. Lett. **63** (1989) 1562; P. Carruthers, H. C. Eggers and I. Sarcevic, Phys. Rev. **C44** (1991) 1629.

[14] W. N. Zhang, Y. M. Liu, S. Wang, Q. J. Liu, J. Jiang, D. Keane, Y. Shao, S. Y. Chu and S. Y. Fung, Phys. Rev. **C47** (1993) 795.

[15] S. Pratt, Phys. Lett. **B301** (1993) 159.

[16] S. Pratt, Phys. Rev. **C50** (1994) 469.

[17] J. D. Bjorken, Phys. Rev. **D27** (1983) 1327.

[18] H. C. Eggers, P. Lipa, P. Carruthers and B. Buschbeck, Phys. Rev. **D48** (1993) 2040.

[19] S. E. Koonin, Phys. Lett. **B70** (1977) 43; F. B. Yano and S. E. Koonin, Phys. Lett. **B78** (1978) 556.

[20] R. Lednicky and V. L. Lyuboshitz, Sov. J. Nucl. Phys. **35** (1982) 770.

Figure 1: Source model picture for the production of two identical bosons.

Figure 2: Correlation between space-time and momentum rapidities of neutral pions calculated in the parton-string model for central $O + O$ collisions at initial energy 200 AGeV.

Figure 3: Correlation functions of two neutral pions calculated in the parton-string model for central $O+O$ and $S+S$ collisions at initial energy 200 AGeV. The meaning of the various points is explained in the text.

Figure 4: The pure correlation functions (only the last term in Eq. (63)) of three neutral pions calculated in the parton-string model for central $O + O$ and $S + S$ collisions at initial energy 200 AGeV.

Figure 5: Multiplicity distributions of neutral pions calculated in the parton-string model for central $O + O$ collisions at initial energy of 200 AGeV. Results with and without inclusion of BE correlations are shown by full and open circles, respectively. The full curve represents the fit of the multiplicity distribution by a superposition of five Poissonians, the dashed curve is obtained from this fit after the inclusion of the BE weights.

Figure 6a: Transverse momentum distributions of neutral pions (left) and their ratios (right) calculated in the parton-string model for central $O + O$ ($n_{\pi^0} = 30, 60$) collisions at initial energy 200 AGeV. The distributions with and without inclusion of BE correlations are shown by full and open circles, respectively.

Figure 6b: The same as in Fig. 6a, but for rapidity distributions.

Figure 6c: The same as in Figs. 6a and 6b, but for central $S + S$ ($n_{\pi^0} = 100$) collisions at initial energy 200 AGeV.

Figure 7: The ratio of the renormalized correlation functions of two neutral pions $C_n(q_{inv})/\omega(n)$ and $C_2(q_{inv})/\omega(2)$ calculated in the parton-string model for central $O + O$ collisions with fixed π^0 multiplicities $n = 30$ and 60 at $E_{lab} = 200$ AGeV.

Figure 8: The two-particle (Eq. (29)) and the pure three-particle (only the last term in Eq. (63)) correlation functions of positively charged pions calculated with (full circles) and without (open circles) the Coulomb penetration factors (left) and their ratios (right) for central $S + S$ collisions simulated within the parton-string model at $E_{lab} = 200$ AGeV.

The source model picture of the two-boson emission

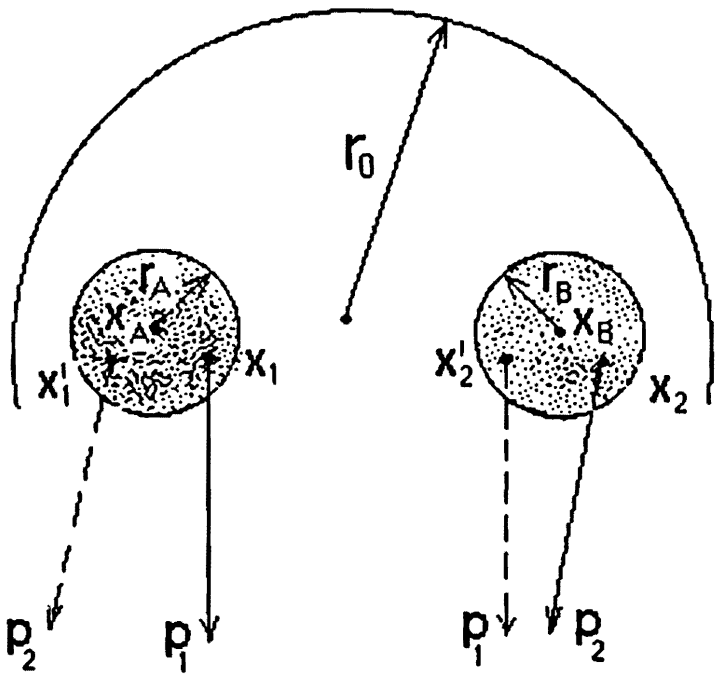

Fig. 1

Central O+O collisions at 200 AGeV

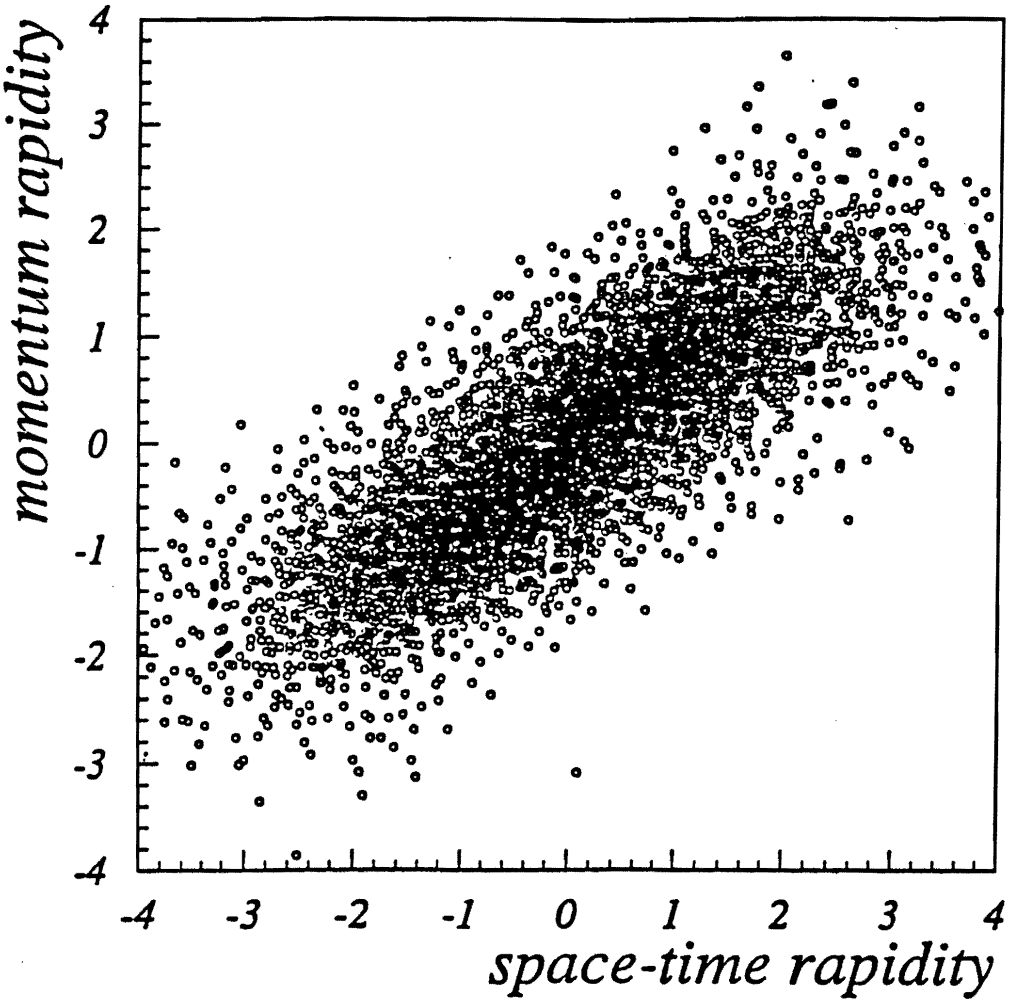

Fig. 2

Central A+A at 200 AGeV

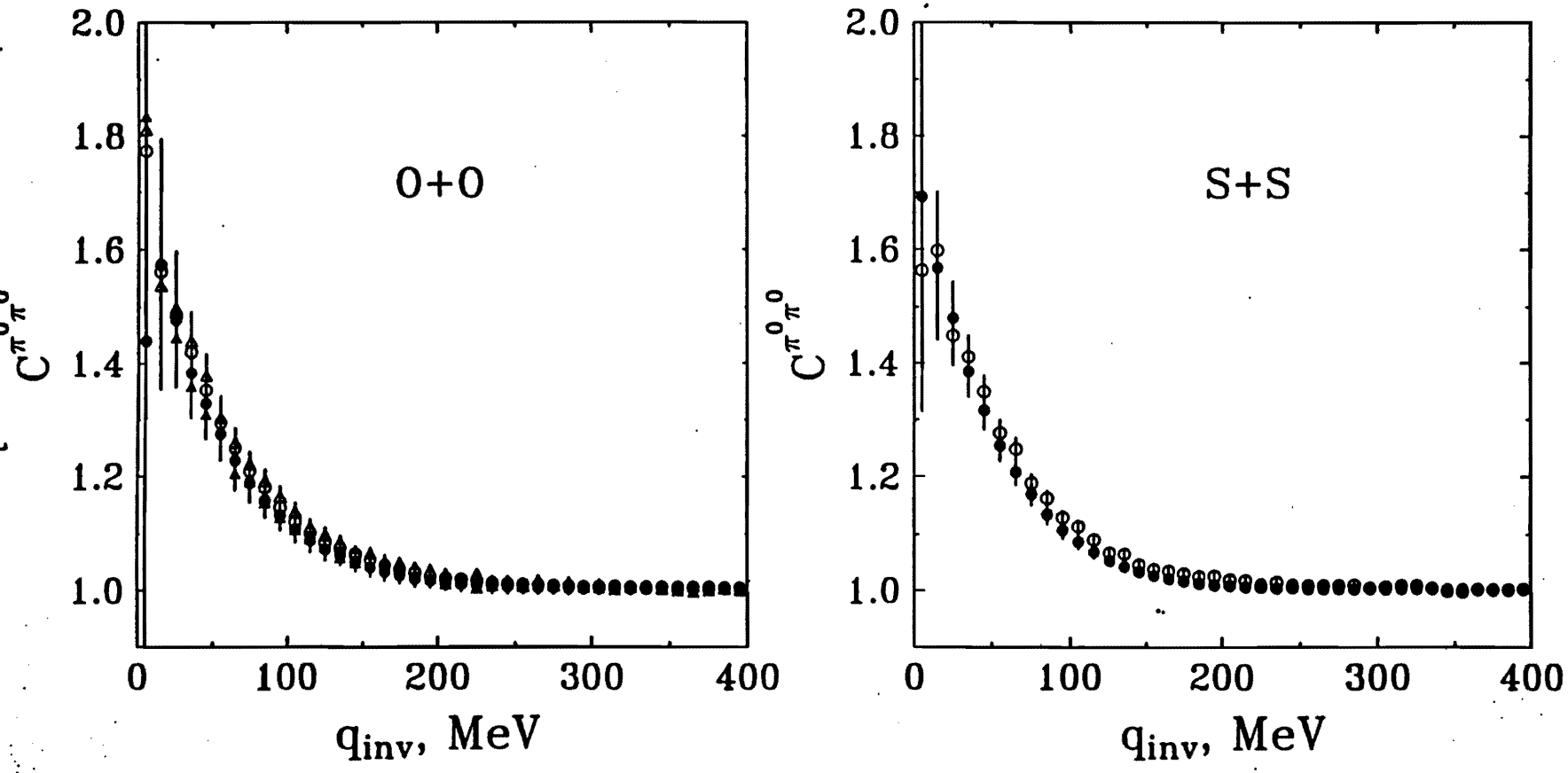

Fig. 3

Central A+A at 200 AGeV

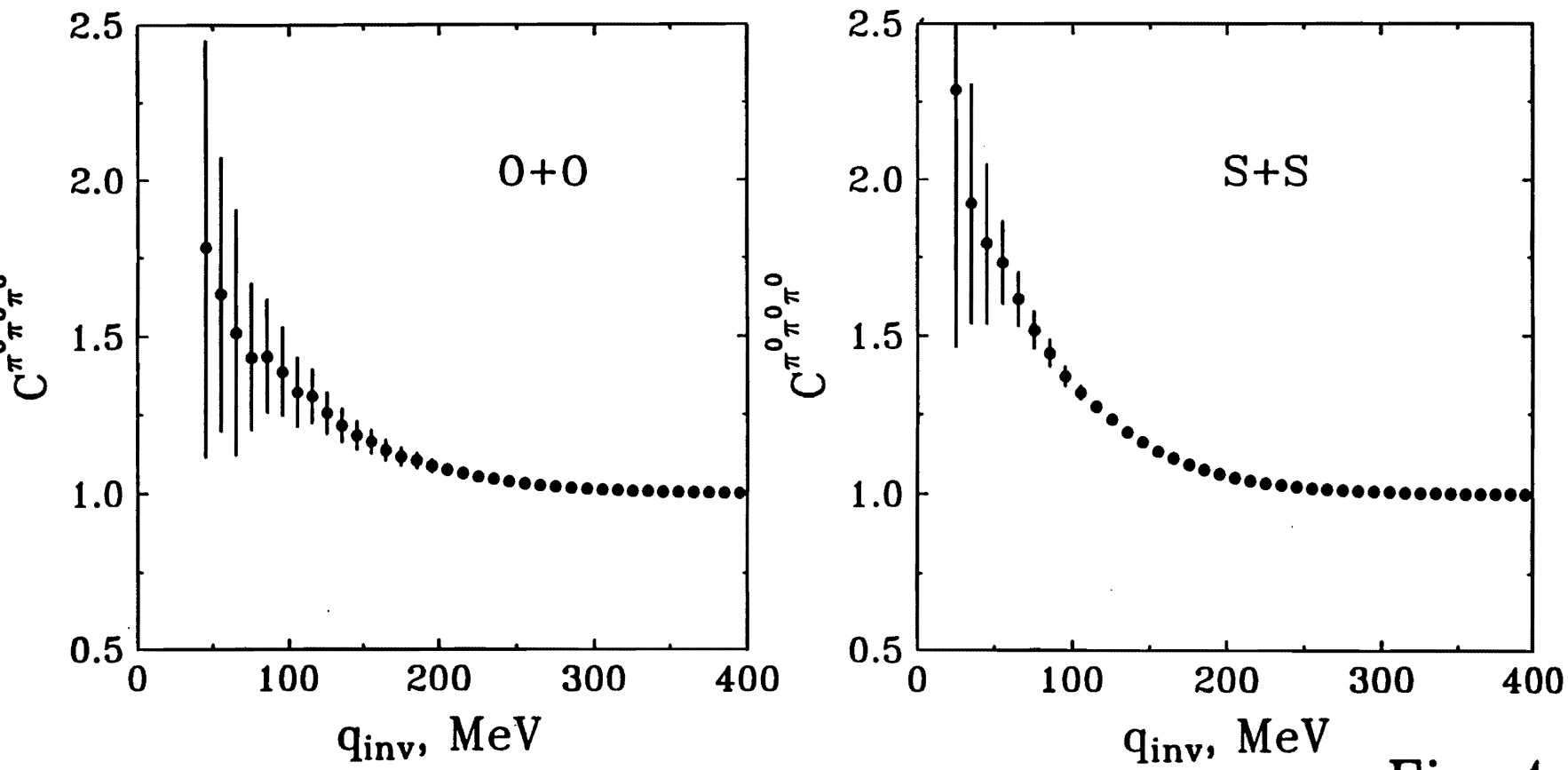

Fig. 4

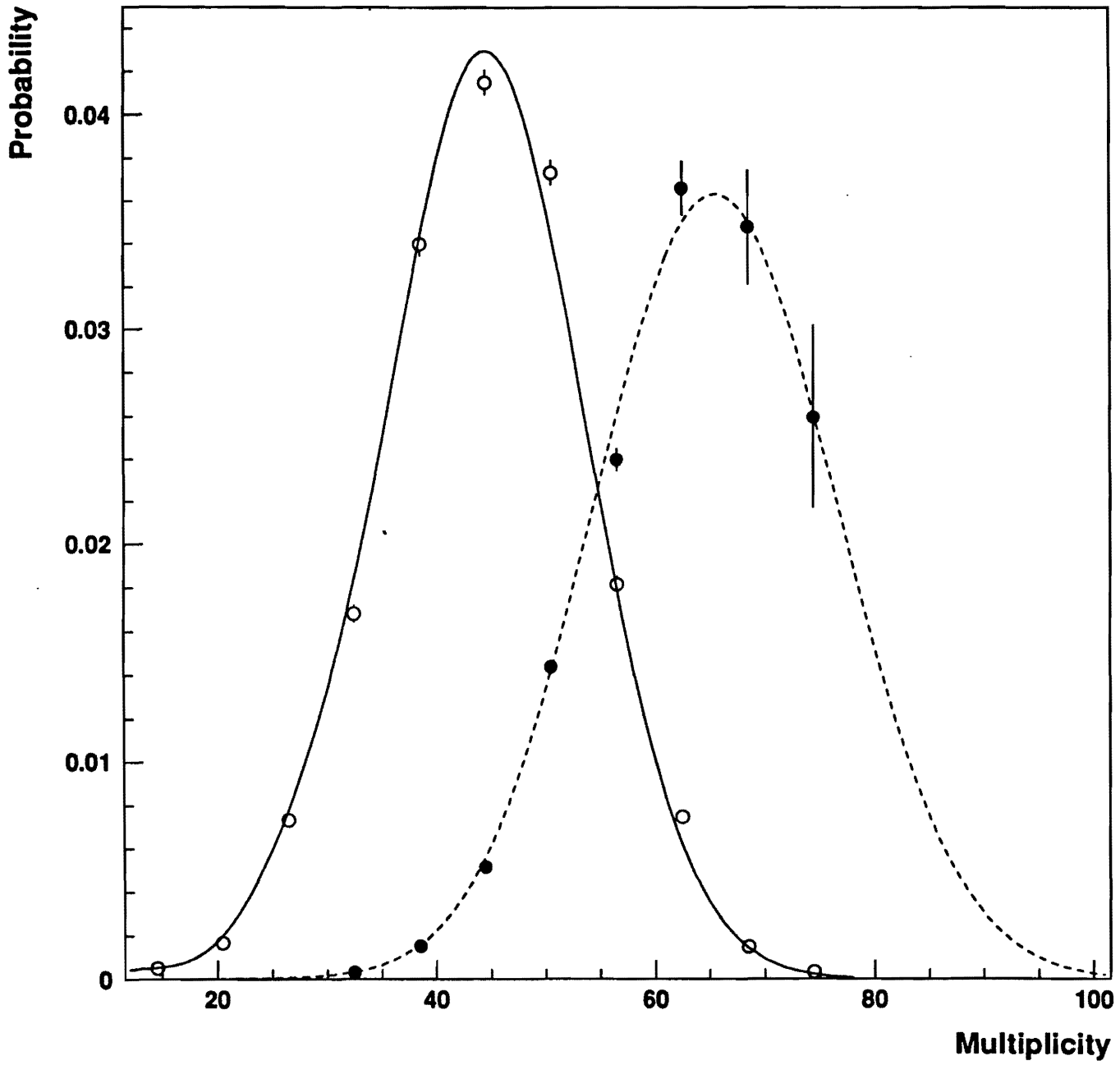

Fig. 5

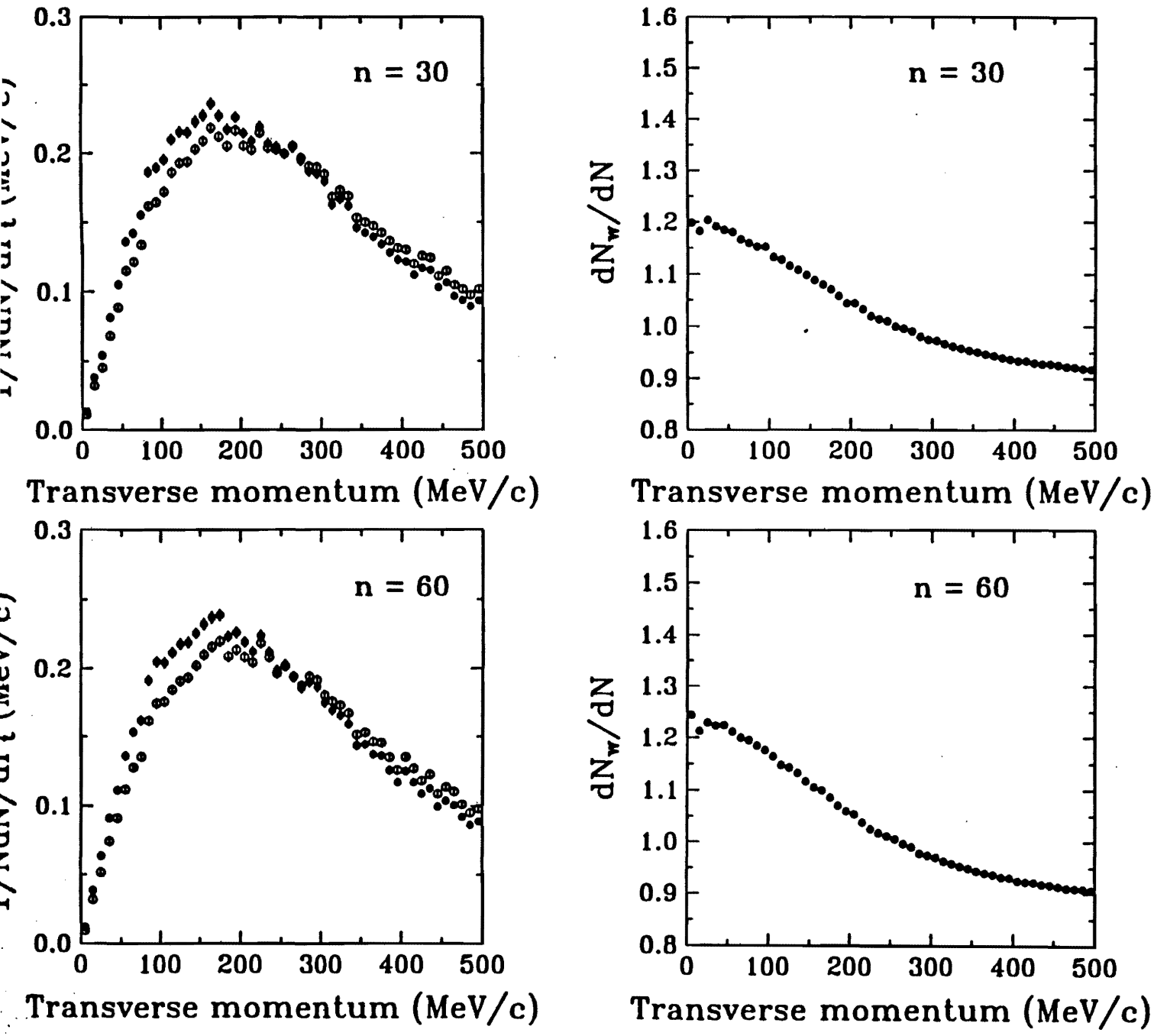
n = 30
n = 60
Transverse momentum (MeV/c)
dN_w/dN
0.0
0.1
0.2
0.3
0.8
0.9
1.0
1.1
1.2
1.3
1.4
1.5
1.6
0
100
200
300
400
500

Fig. 6a

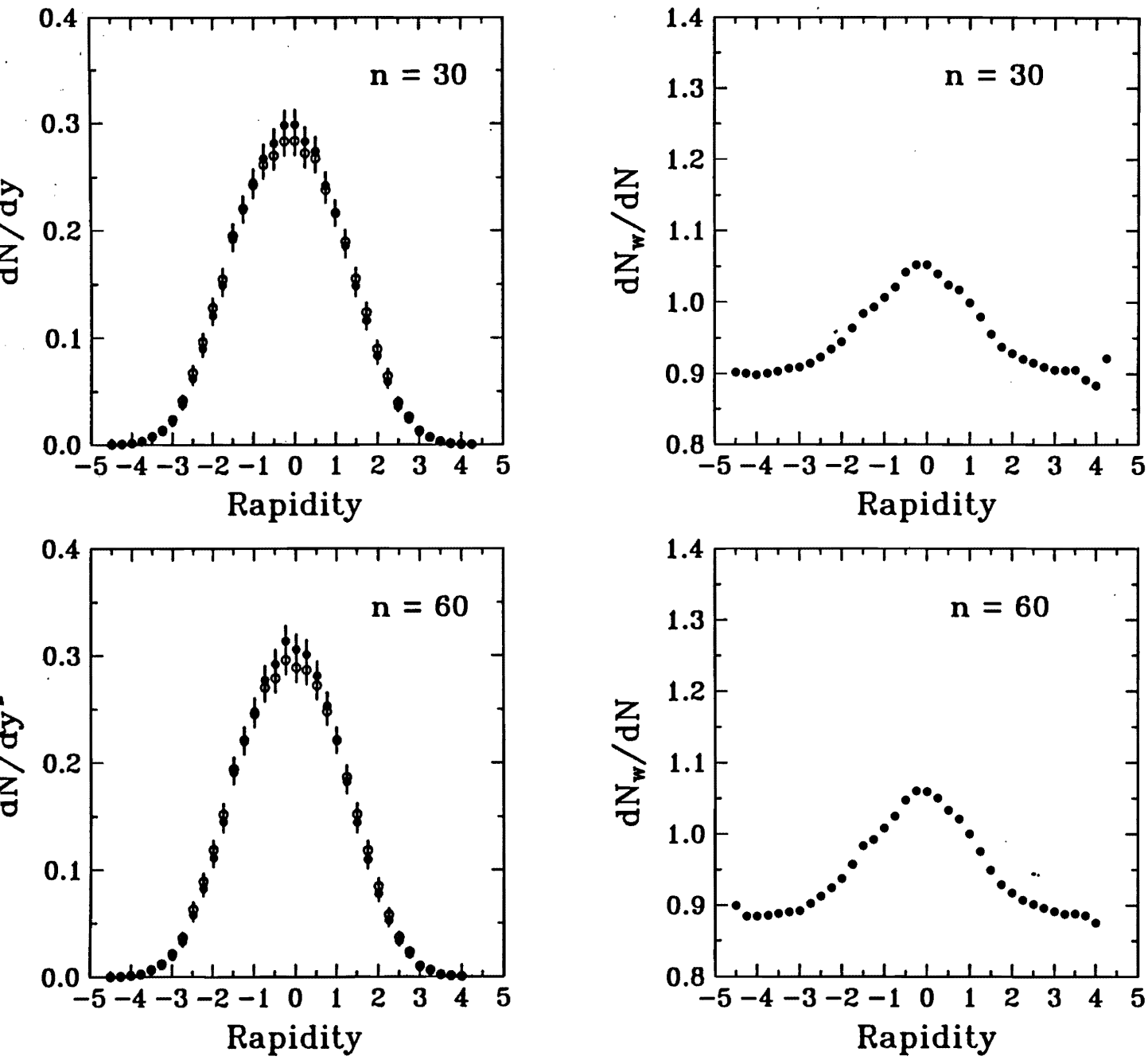
n = 30
dN/dy
Rapidity
n = 30
dN_w/dN
Rapidity
n = 60
dN/dy
Rapidity
n = 60
dN_w/dN
Rapidity

Fig. 6b

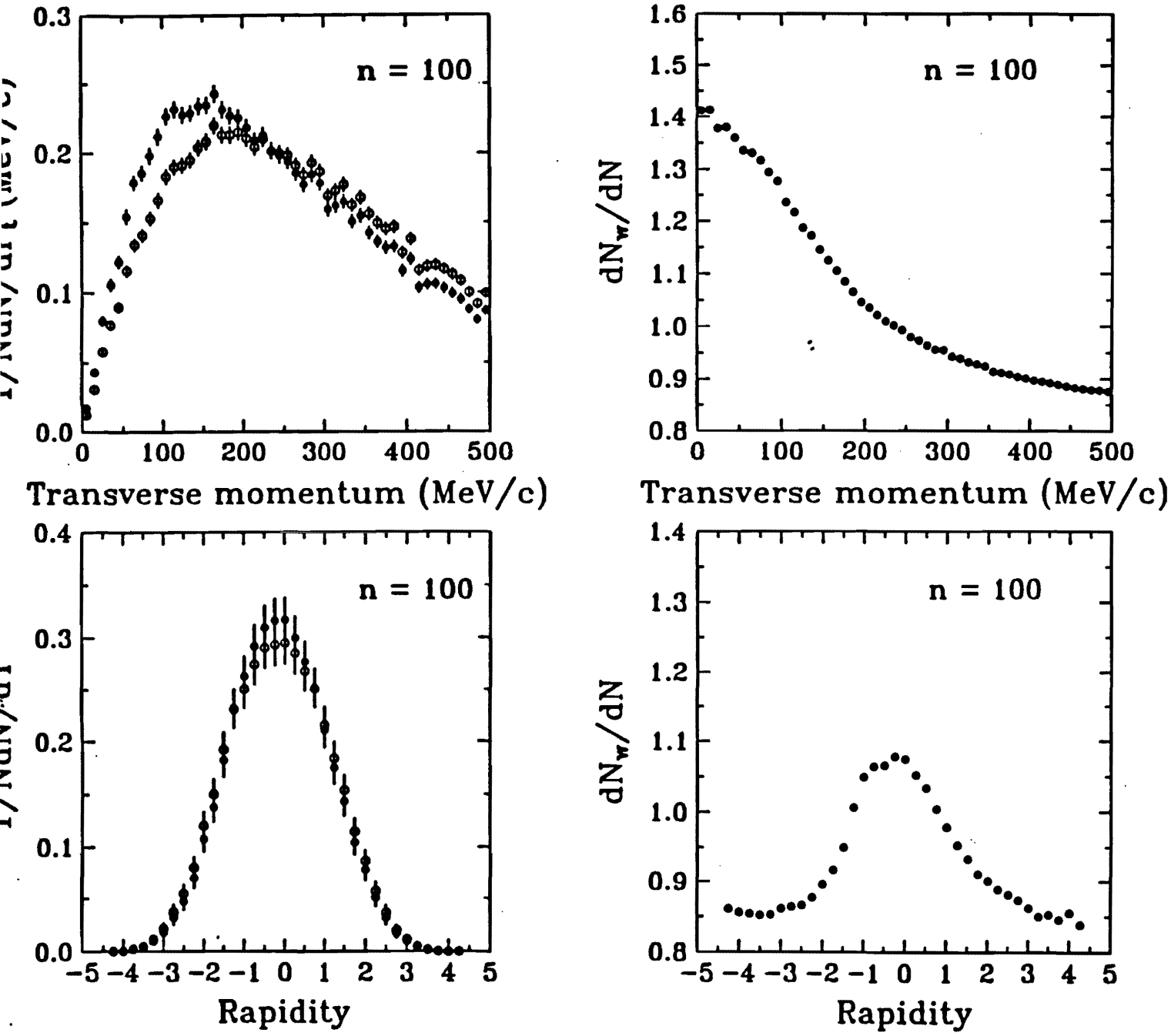
n = 100
Transverse momentum (MeV/c)
n = 100
dN_w/dN
Transverse momentum (MeV/c)
n = 100
Rapidity
n = 100
dN_w/dN
Rapidity

Fig. 6c

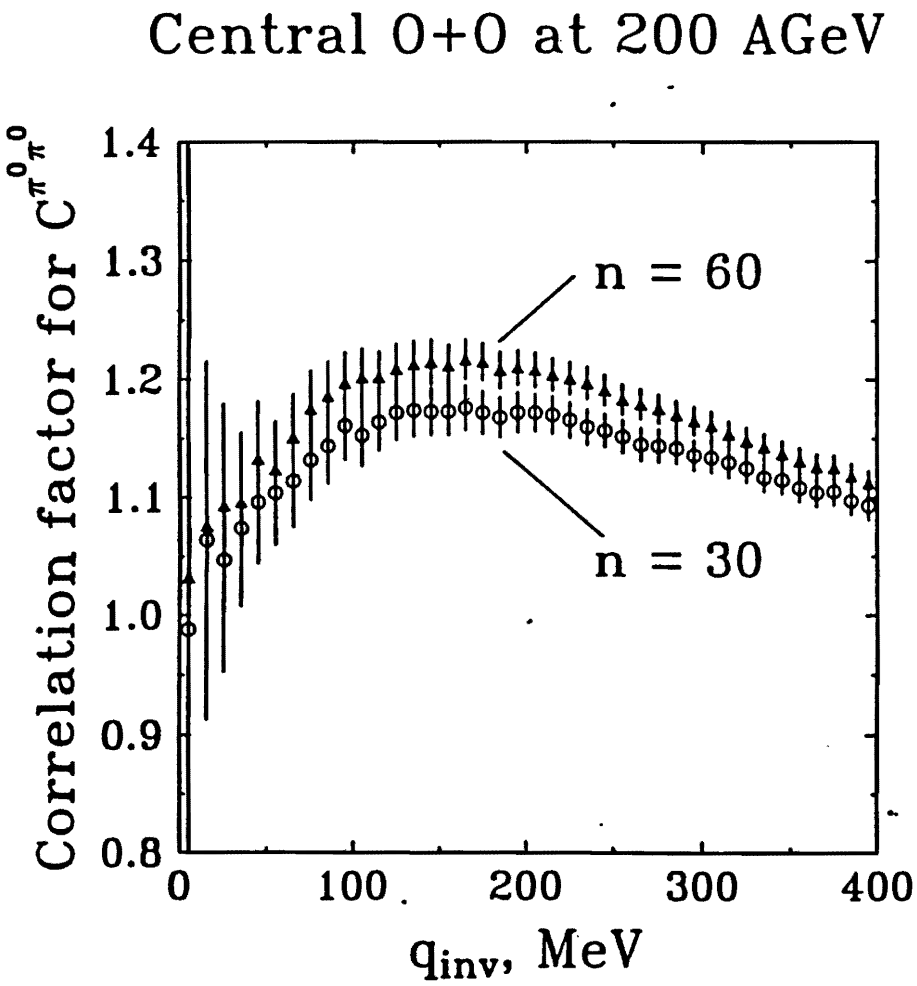
Central O+O at 200 AGeV
Correlation factor for $C^{\pi^0\pi^0}$
1.4
1.3
1.2
1.1
1.0
0.9
0.8
0
100
200
300
400
q_{inv}, MeV
n = 60
n = 30

Fig. 7

Central S+S at 200 AGeV

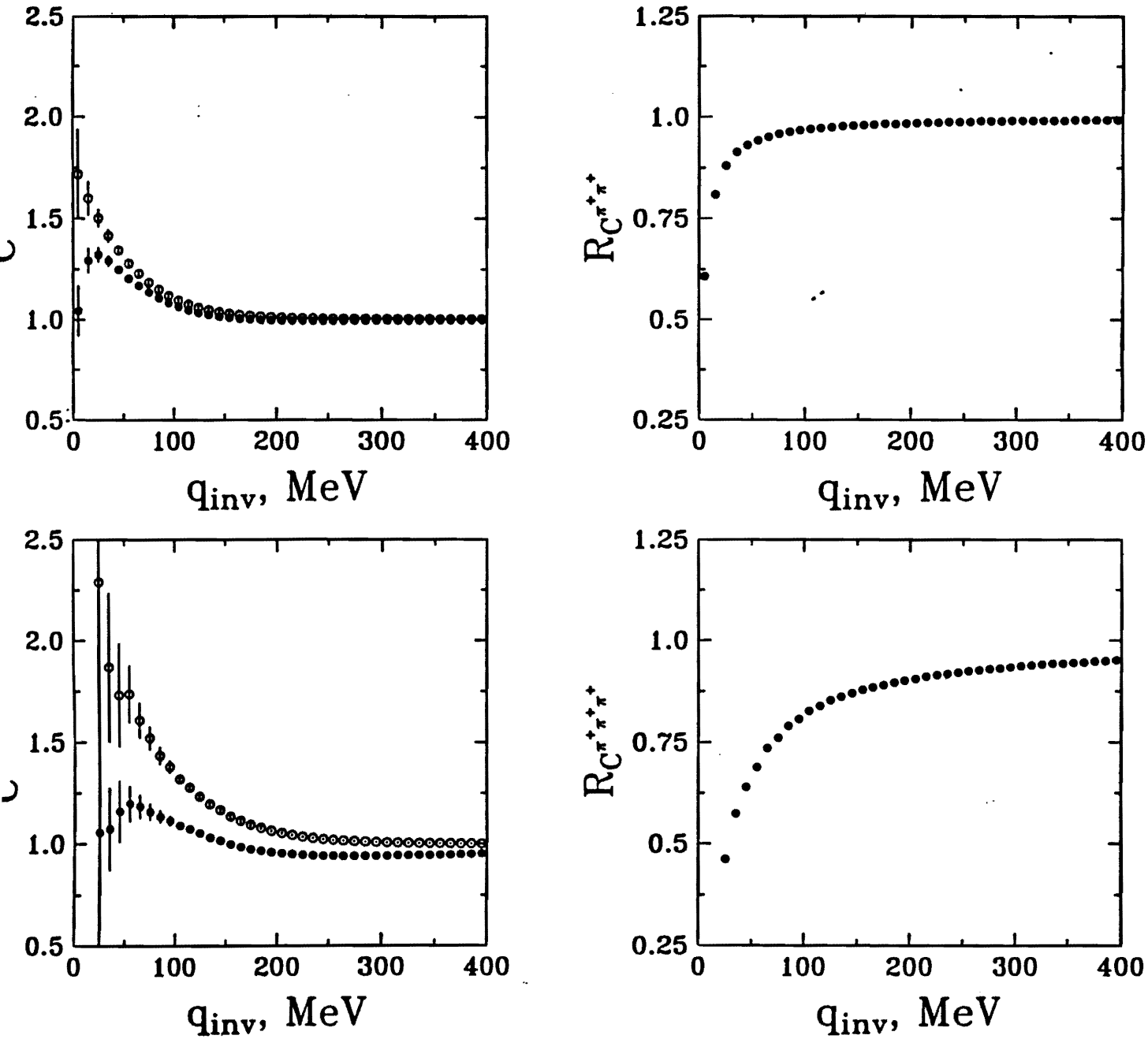

Fig. 8